AD-A092 876 TEXAS INSTRUMENTS INC DALLAS F/G 9/5
ACOUSTIC SURFACE WAVE RESONATORS AND FILTERS ON ST QUARTZ.(U)
DEC 77 W R SHREVE N00173-76-C-0338
UNCLASSIFIED TI-08-77-51 NL

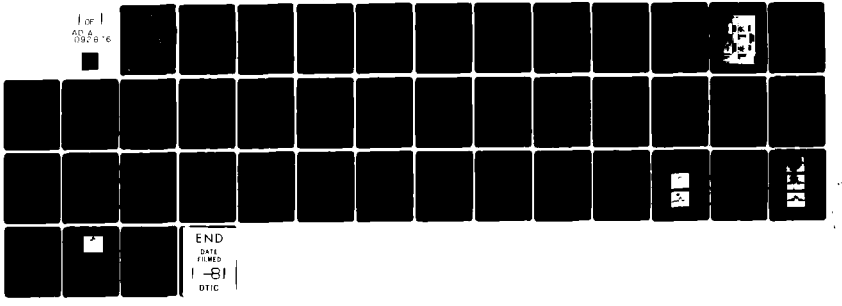

END
DATE FILMED
1-81
DTIC

LEVEL II

(2)

ACOUSTIC SURFACE WAVE RESONATORS AND FILTERS ON ST QUARTZ

Texas Instruments Incorporated
13500 North Central Expressway
Dallas, Texas 75222

December 1977

Final Report for Period September 1976 to December 1977

Naval Research Laboratory
Washington, D.C. 20375

UNCLASSIFIED

SECURITY CLASSIFICATION OF THIS PAGE (When Data Entered)

REPORT DOCUMENTATION PAGE

READ INSTRUCTIONS BEFORE COMPLETING FORM

1. REPORT NUMBER	2. GOVT ACCESSION NO. AD-A073 876 / 3. RECIPIENT'S CATALOG NUMBER
4. TITLE (and Subtitle) Acoustic Surface Wave Resonators and Filters on ST Quartz	5. TYPE OF REPORT & PERIOD COVERED Final Report September 1976–December 1977
	6. PERFORMING ORG. REPORT NUMBER 08-77-51
7. AUTHOR(s) William R. Shreve	8. CONTRACT OR GRANT NUMBER(s) N00173-76-C-0338
9. PERFORMING ORGANIZATION NAME AND ADDRESS Texas Instruments Incorporated 13500 North Central Expressway Dallas, Texas 75222	10. PROGRAM ELEMENT, PROJECT, TASK AREA & WORK UNIT NUMBERS
11. CONTROLLING OFFICE NAME AND ADDRESS Naval Research Laboratory Washington, DC 20375	12. REPORT DATE December 1977
	13. NUMBER OF PAGES
14. MONITORING AGENCY NAME & ADDRESS (if different from Controlling Office)	15. SECURITY CLASS. (of this report) Unclassified
	15a. DECLASSIFICATION/DOWNGRADING SCHEDULE

16. DISTRIBUTION STATEMENT (of this Report)

Reproduction in whole or in part is permitted for any purposes of the United States Government

APPROVED FOR PUBLIC RELEASE
DISTRIBUTION UNLIMITED

17. DISTRIBUTION STATEMENT (of the abstract entered in Block 20, if different from Report)

18. SUPPLEMENTARY NOTES

19. KEY WORDS (Continue on reverse side if necessary and identify by block number)

resonator aging
quartz resonator
surface acoustic wave–resonators
surface acoustic wave–filters
aging processes
resonator tuning
high-Q resonators
loss in resonators

20. ABSTRACT (Continue on reverse side if necessary and identify by block number)

The objective of this program is to maximize the usefulness of surface acoustic wave (SAW) resonators for applications to filter and oscillator circuits. This program focuses on improving fabrication to yield the lowest possible aging rate, designing a 70-MHz resonator to achieve the highest possible Q, and examining the use of resonators at higher frequencies with a 600-MHz filter.

The program was divided into three sections: aging studies, high-Q studies, and a high-frequency study. In the area of aging, the results of a previous study ~~under Contract N00013-75-0824~~ with the Office of Naval Research were used to determine the optimum fabrication and mounting procedure for SAW resonators. The goal of this work was to

DD FORM 1 JAN 73 1473A EDITION OF 1 NOV 65 IS OBSOLETE

UNCLASSIFIED

SECURITY CLASSIFICATION OF THIS PAGE (When Data Entered)

determine the aging rate for resonators made in this manner and to determine the effect of elevated temperatures on this rate. This data would then be used to determine the best preaging cycle to obtain long term stable operation. In addition, the effects of tuning with ZnO and of an arbitrary preaging cycle were measured.

In the high-Q studies, the sources of loss in the resonator were analyzed and an approach was identified to achieve the contract goals. The devices built under this contract do not meet the contract goals, but the sources of additional loss have been identified. The devices built under this section have been made into one-pole filters. Additional work to achieve high Q was curtailed when the contract was not fully funded.

No work was performed on high-frequency devices that incorporate the advances made in the high-Q study because of incomplete funding of this contract.

The aging study showed that current resonator fabrication and packaging leads to a device aging rate of −13 ppm per year after preaging for 4 months. This rate increases slightly with temperature. After 6 months of preaging, the aging rate is below −10 ppm per year up to 100°C. From 150° to 250°C, this rate increases from −12 ppm per year to −160 ppm per year. From this data and an observed degradation in insertion loss above 150°C, it can be concluded that operation above 150°C should be avoided. The data on aging of ZnO tuned resonators shows an acceleration by a factor of 3 caused by tuning. Thus, a better tuning technique for grooved quartz resonators is needed. For lower aging rates, new cleaning, mounting, and packaging techniques should be investigated. The area of SAW resonator cleaning, mounting, and packaging for low aging is ripe for further research.

The high-Q results show that the loss mechanisms in grooved quartz resonators are well understood, but further effort is needed in the area of reflector weighting for bulk scattering suppression and for improved filter out-of-band rejection. The filters built under this study exhibited a maximum Q of 40,000 in vacuum. The out-of-band rejection was degraded by a spurious resonance and direct coupling between matching inductors, a packaging problem.

1473 B

TABLE OF CONTENTS

Section	*Title*	*Page*
I	AGING STUDIES	3
	A. Step-Stress Results	3
	B. Fabrication	5
	C. Experimental Setup and Test Procedure	7
	D. Test Results	11
	E. Frequency Data Analysis	18
	F. Conclusions	26
II	HIGH-Q STUDIES	27
	A. Loss Analysis	27
	1. Air Loading Loss	27
	2. Viscuous Material Loss	28
	3. Scattering Into Bulk Waves	28
	4. Transducer Loss	30
	5. Reflection Loss	31
	6. Surface Scattering	31
	B. High-Q Resonator Design	32
	C. Experimental Results	34
	1. Q Measurements	34
	2. Jogged Transducers	34
	3. Multimode Response	38
	D. Deliverable Devices	38
	E. Conclusions	40

LIST OF ILLUSTRATIONS

Figure	*Title*	*Page*
1	Frequency Changes Due to Step-Stress and Isothermal Aging	4
2	Frequency Changes of Etched Devices Referenced After Preaging	6
3	Typical Resonator Characteristics	8
4	Oscillator Schematic	9
5	Resonator Amplitude and Phase Response	9
6	Oscillator Block Diagram	10
7	Resonator Frequency Versus Aging Time	12
8	Resonator Frequency Versus Logarithm of Aging Time	14
9	Resonator Insertion Loss Versus Aging Time	16
10	Resonator Bandwidth Versus Aging Time	19
11	Resonator Unloaded Q Versus Aging Time	21
12	Effect on Frequency of Aging Resonators at 22°, 50°, 100°, 150°, 200°, and 250°C Least Squares Data Fit	25
13	Effect on Frequency of Aging Resonators at 22°, 50°, 100°, 150°, 200°, and 250°C Extrapolation From Least Squares Data Fit	25
14	Array Weighting Functions for Suppression of Scattering Into Bulk Waves	31

15 Resonator Schematic 33
16 Jogged Transducer Delay Line Frequency Responses 35
17 Resonator Frequency Response 37
18 Frequency Response of Filter 7 39
19 Package and Bonding Diagram for One-Pole Filters 39

LIST OF TABLES

Table *Title* *Page*

1 Data Fit to A Log (1 + Bt) + C $\cdot$(1 $-$ e^{Dt}) 24
2 Loss And Q at 70 MHz 28
3 Bulk Scattering Suppression 30
4 Measurements on Resonators With 0.013-Wavelength-Deep Grooves 35
5 Measurements in Air on Resonators With 0.020-Wavelength-Deep Grooves 36
6 Comparison of Experimental and Theoretical Q 36
7 Deliverable Filter Characteristics 38

SECTION I
AGING STUDIES

The purposes of this study are to determine the effect of fabrication processes on the aging of ST quartz resonators and to obtain a meaningful extrapolation of aging rates at elevated temperatures to long-term room temperature aging. The steps used to fabricate devices for this aging study are described. The results of the step-stress study completed under this contract are described to illustrate the considerations that went into the design of the current aging experiment. The fabrication and testing of devices is described, followed by the test results, analysis and extrapolation of these results, and a summary of conclusions and recommendations for further study.

A. STEP-STRESS RESULTS

The aging studies started under Contract No. N00014-75-C-0824 have been completed, and the results have been analyzed. The details of this work are presented in the final report.[1] The step-stress portion of this study is described here to illustrate the factors that affected the setup of the current aging experiment. The step-stress work was completed under the current contract, but all results are included in the final report for the previous contract.

Four lots of devices were tested to evaluate the effects on aging of a post-polish chemical etch. This etch was intended to eliminate the amorphous surface layer that is left after polishing. Also, additional cleaning steps were evaluated. The tests consisted of both step-stress and isothermal aging. Half the devices were made from a polished slice that had been lightly etched in concentrated HF (15 seconds at room temperature) after polishing. The other half of the devices were made from a slice treated identically except that the etch step was omitted. Each group was divided again on the basis of the cleaning procedure following deblocking after dicing. In the "standard cleaning" case, the standard organic solvent procedures were used. In the "clean" case, additional swabbing and soaking were used to assure the maximum possible device cleanliness.

The step-stress part of the experiment consisted of measuring the device performance at room temperature and after 16 hours at each elevated temperature (100°, 150°, 200°, and 250°C). Since one set of measurements can be made each day, the work load is constant and the duration of the experiment is well known. The results are shown in Figure 1, including the first data point at 250°C. It is clear from just the easily obtained step-stress data that there are significant differences between the lots tested.

The aging tests were continued isothermally to help evaluate the significance of the differences found during the step-stress tests. After one day at 250°C, all devices appeared to be quite stable. At 4 days, the devices were sealed in dry nitrogen. Before the devices reached a new equilibrium, frequency shifts were observed. As the curves show, the devices that received extra cleaning reached their new equilibrium more slowly.

[1] D.T. Bell, Jr., "Acoustic Surface Wave Resonators and Filters on ST Quartz," Final Report, Contract No. N00013-75-C-0824, Office of Naval Research.

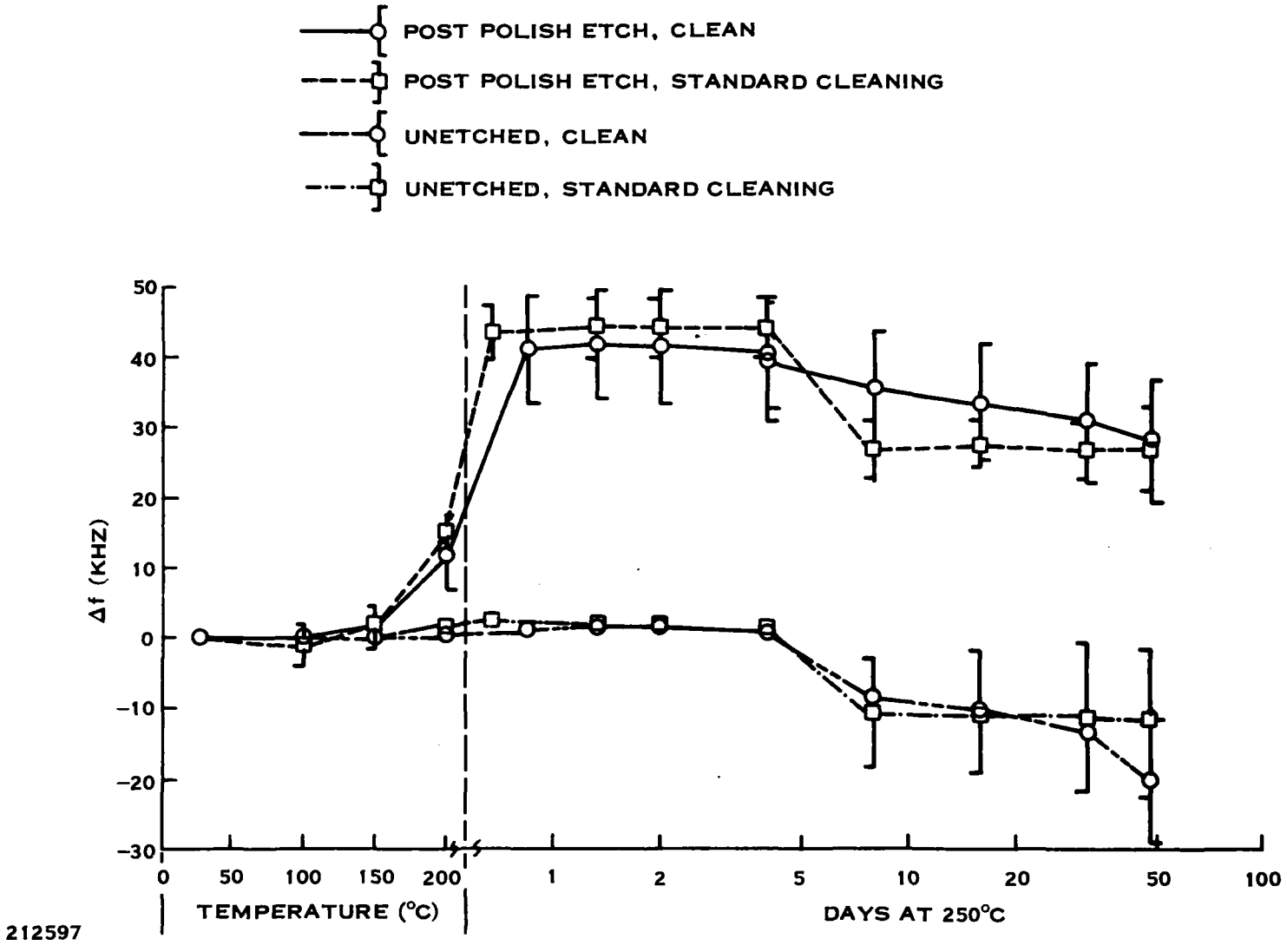

Figure 1. Frequency Changes Due to Step-Stress and Isothermal Aging

The same data can be viewed in a different manner by considering the aging before one day at 250°C as a preaging cycle. The reference frequency becomes the frequency after this preage cycle. The data on the etched devices with this new reference are shown in Figure 2. The reference point ($\Delta f = 0$) is marked with an X. The small deviations between 1 and 4 days may be predicted from a computer analysis of the change per step rather than the cumulative change plotted here. Note that the frequency is stable to ±1 kHz including the standard deviations (<0.3 kHz when not indicated).

At 4 days, the packages were sealed. Before this, the aging took place in an oven supplied with a positive flow of dry nitrogen. After sealing, the aging changed rapidly, indicating the initiation of a new process not stabilized by the earlier aging. This process probably is the adsorption of gases from the mounting material and package surfaces which are now confined to the package. Thus, a useful preaging schedule cannot effectively be completed until after the last fabrication step on the resonator.

Examination of Figures 1 and 2 shows that the cleaning process has an important impact on the post-seal aging. The conventionally cleaned devices change rapidly but then stabilize at a new frequency. The explanation for this difference is not certain, but is probably due to the smaller surface damage suffered by these devices.

B. FABRICATION

The fabrication process and aging test procedures for the current study are based on results from the aging tests performed under Contract No. N00014-75-C-0824. Standard resonator cleaning and fabrication processes[1] are used with the addition of a noncontact final cleaning step (rf plasma asher cleanup) to remove residual organic contamination. Between fabrication steps, including mounting and bonding, the devices are stored in dry boxes with a positive flow of dry nitrogen. This atmosphere is maintained during a presealing aging cycle of 4 days at each of the lower aging temperatures and 1 day at the two highest temperatures; the ovens used are supplied with positive flow of dry nitrogen.

Two-inch-square commercial ST cut (42.75-degree rotated-y cut) quartz wafers were purchased for this study. They were polished with a chemical-mechanical process using Syton. After solvent cleaning, 1,000 Å of aluminum was vacuum deposited on the preheated substrates. The resonator patterns were defined photolithographically and the aluminum was etched to form the transducers. The reflector arrays were plasma etched[2] into the quartz to a depth of 1,300 Å. The resist was removed and the wafers were mounted for sawing. After sawing, the mounting wax was removed with solvents and the devices were given a final noncontact plasma asher cleanup to remove residual organic contamination. After this time, the devices were stored in flowing dry nitrogen boxes until they were sealed.

The devices were mounted on a gold plated TO-8 header with a small dot of Dow Corning 6-1104 RTV and thermal compression ball bonded with 1-mil gold wire. The RTV bonding material was used to eliminate stress induced frequency changes caused by thermal cycling during the aging program. This RTV is space qualified and has a particularly low content of condensable volatile material. Devices mounted with this material were shown to age more slowly than

[2]S.P. Miller, R.E. Stigall, and W.R. Shreve, "Plasma-Etched Quartz SAW Resonators," *1975 Ultrasonics Symp. Proc.*, IEEE Pub. No. 75 CHO 994-4SU (September 1975), pp. 474–477.

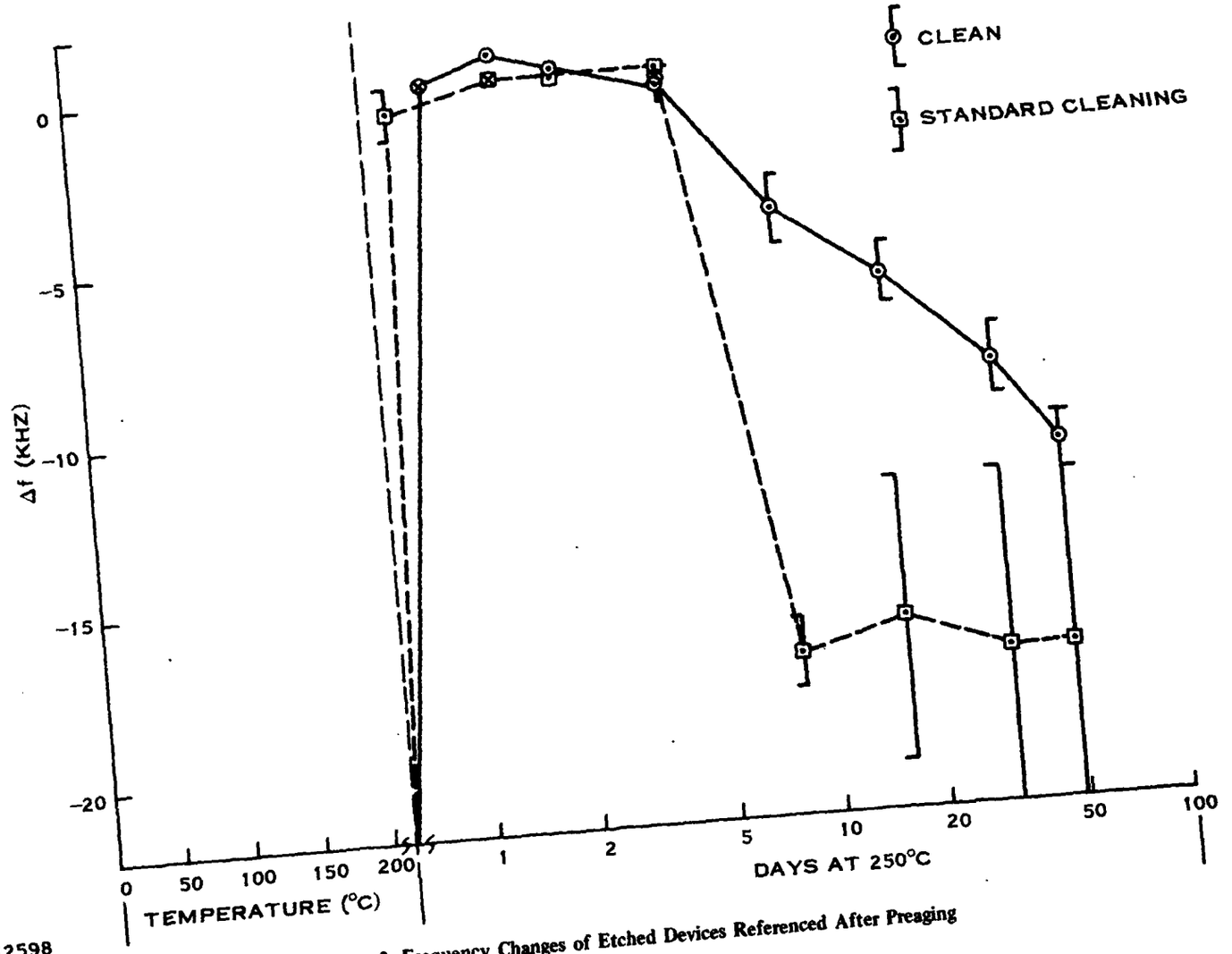

212598

Figure 2. Frequency Changes of Etched Devices Referenced After Preaging

devices mounted with other low outgassing materials in the previous study. In that study, the lower aging rate was predicted from thermal gravimetric analysis of the mounting materials. No material stood up well at 250°C in either the isothermal or step-stress aging tests. The gravimetric analysis showed little change in the 6-1104 RTV below 200°C. It was chosen as the best available material for these tests. After curing the RTV and cycling the devices to their respective aging temperatures as described below, they were back filled with dry nitrogen and sealed by seam welding lids on the headers.

A device that is typical of those used in this study is shown in Figure 3. The top of the figure shows the device and a closeup of the groove reflector in cross section. The grooves on the device photograph appear bright because light is diffracted from the array. The bonding pads for the transducers appear as black areas on the edges of the device. Extra transducers are visible at the ends of the device. They were not used in these tests. The frequency response of this device in a 50-ohm system using the center transducers is shown in the bottom of Figure 3. Initially, the average insertion loss was 11.9 dB at an average frequency of 194.41 MHz with an average 3-dB bandwidth of 15.8 kHz. The average unloaded Q was 16,000.

C. EXPERIMENTAL SETUP AND TEST PROCEDURE

One hundred and sixty devices were fabricated and divided into eight groups of 20 devices each. Six of these groups were aged isothermally at room temperature, and at 50°, 100°, 150°, 200° and 250°C. Another group was tuned down in frequency by approximately 250 parts per million with a dielectric overlay of zinc oxide. This group was preaged for 36 days at 150°C and then isothermally aged at 100°C. The last group was preaged at 150°C for 36 days and then isothermally aged at room temperature.

All of the devices aged at 50°, 100°, and 150°C were aged for 4 days at their respective temperature before sealing. The higher temperature groups were aged for only 1 day prior to sealing. The room temperature devices were sealed 11 days after the start of testing. All devices were maintained in a dry nitrogen atmosphere before sealing. Frequency measurements were made at increasing intervals of time by cycling the devices to room temperature. Measurements of center frequency, 3-dB loss points, and absolute insertion loss were made on an HP 8552B, 8554B spectrum analyzer with a model 970 Eldorado frequency counter. This technique gives a best-case experimental uncertainty of ±0.2 kHz or ±1 ppm at 200 MHz.

For greater frequency accuracy and to provide an independent check on the spectrum analyzer results, the oscillation frequency of each device was measured in a feedback oscillator shown schematically in Figure 4. The simplicity of an oscillator circuit with a two-port resonator is the key to its stability. The circuitry was provided with a flow of nitrogen to remove heat and thereby maintain the test socket and resonator near 22°C where the quartz temperature coefficient of delay is zero. A stable oscillator should provide an accurate measure of resonator frequency because of the strong dependence of transmission phase on frequency near resonance. A change in the resonator frequency will cause a like change in the phase and shift the oscillation frequency of the feedback loop. Figure 5 shows the measured frequency response of a typical resonator. The phase slope, $d\phi/d\omega$, is 19 μs corresponding to a frequency change of 0.15 kHz (0.8 parts per million) per degree of phase change. Thus, to achieve 0.1 part per million measurement accuracy, the circuit must be stable to 0.25 degrees of phase shift.

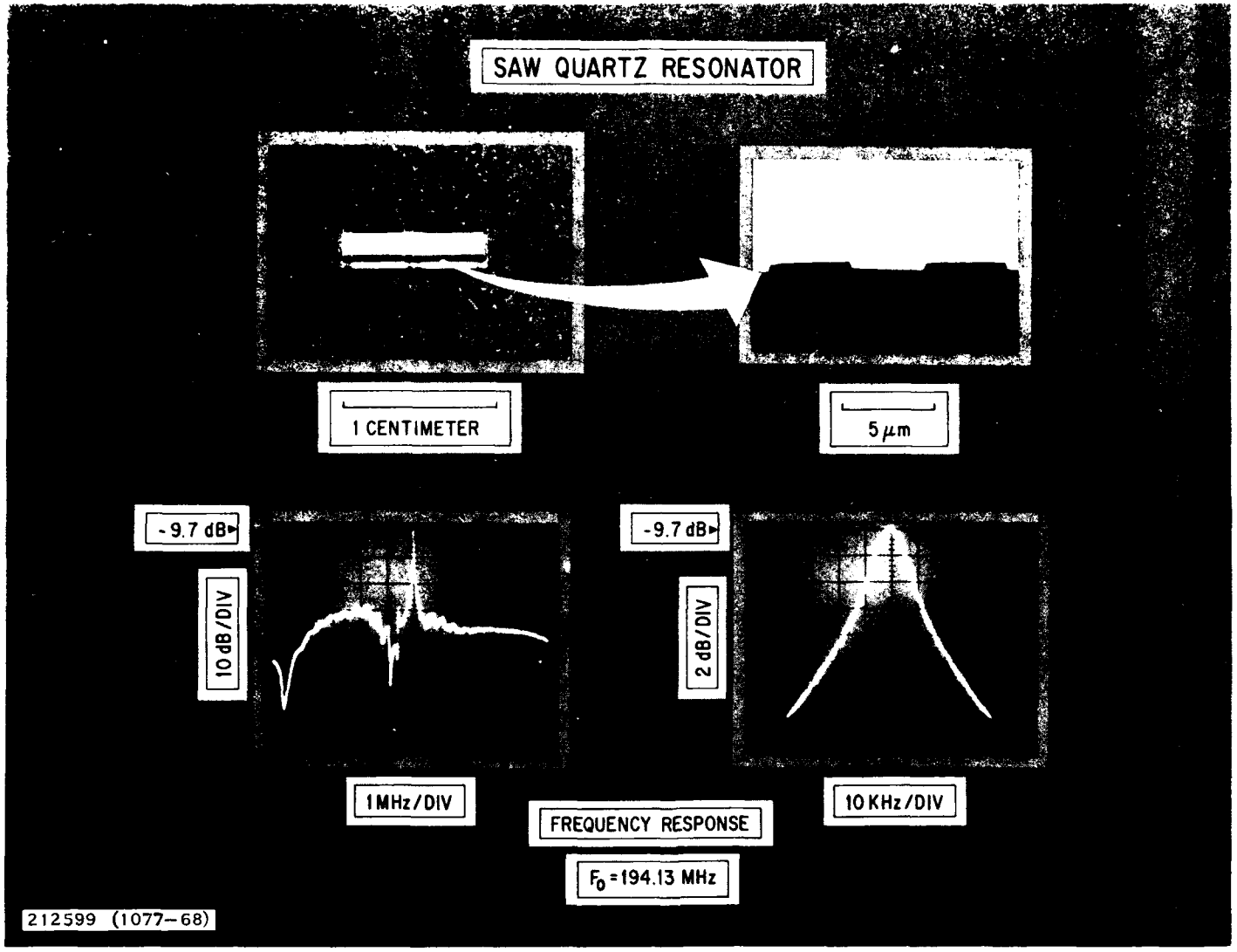

Figure 3. Typical Resonator Characteristics

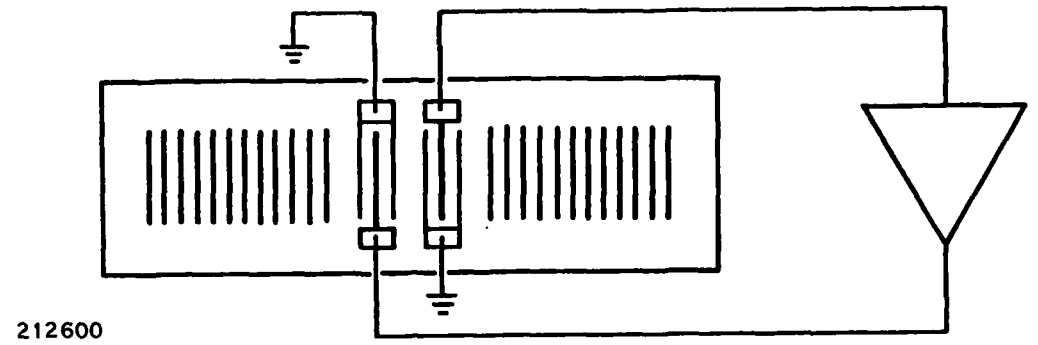

Figure 4. Oscillator Schematic

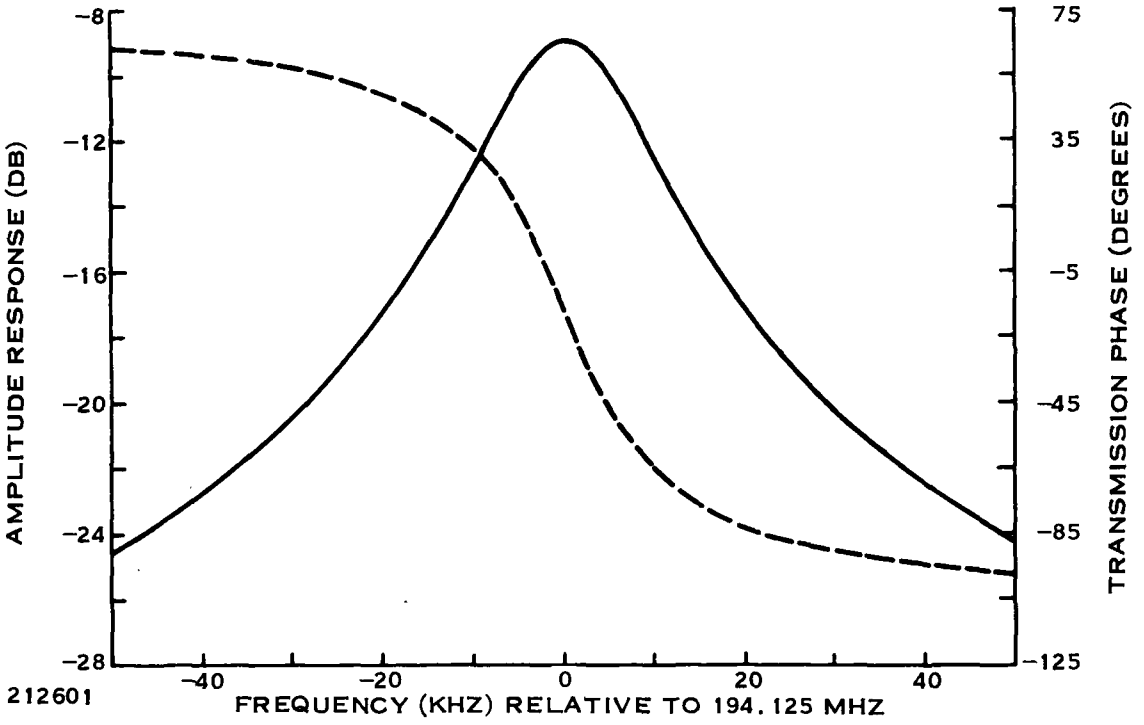

Figure 5. Resonator Amplitude and Phase Response

A block diagram of the circuit used in these tests is shown in Figure 6. The phase adjustment and attenuating pad were adjusted to permit oscillation of a typical resonator as long as the loss remained below 15 dB. All resonators were measured in the same oscillator. A standard TO-8 socket is used to allow convenient interconnection. The oscillator was operated at an elevated temperature for one week prior to taking data to accelerate aging of the oscillator components and thereby minimize their effect on the aging tests. The power supply voltage into

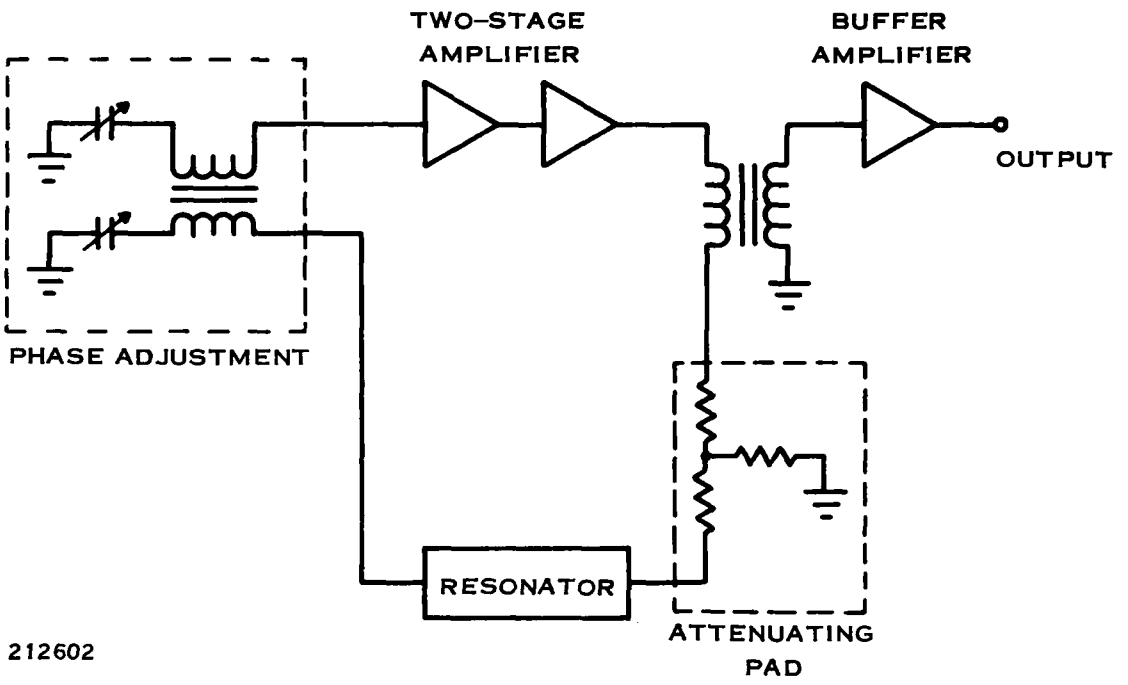

Figure 6. Oscillator Block Diagram

the oscillator is maintained at 12.000 ±0.001 V during the tests and is continuously monitored. A flow of nitrogen is maintained around the circuit components to prevent the transfer of heat to the resonator. This procedure was found to be necessary if the resonator temperature and, therefore, the oscillator frequency were to stabilize quickly (in 1 minute or less).

The major problem with this oscillator technique appears to be maintaining the resonator at the same temperature each time a measurement is made. The test procedure is intended to ensure operation near 22°C, the turnover temperature of the quartz substrate, and thereby to minimize temperature effects. Measurement repeatability was better with the oscillator than for the equivalent spectrum analyzer frequency measurement. Stability of a test resonator measured over a period of several hours was also better than the spectrum analyzer measurement. Both oscillator and spectrum analyzer measurements were taken in this series of tests to examine the long-term accuracy of the oscillator method. The oscillator frequency is affected by factors other than the resonator frequency, such as resonator insertion loss, and therefore may not be the best measurement for aging tests. Results from the two methods are compared in the analysis section.

For further improvement of the accuracy of the frequency measurement, entire oscillators should be built around each resonator and aged as a unit. Measurements could be made at the aging temperature to eliminate temperature cycling effects, or the oscillators could be cycled to room temperature for measurement. In either case, continuous operation would eliminate the warmup changes that have introduced uncertainty in these tests. This procedure was beyond the scope of the current program.

D. TEST RESULTS

From the measured data, the resonator center frequency, bandwidth, insertion loss, unloaded Q, and the oscillator frequency were determined. These data were averaged for each group and the variation of each parameter was analyzed. The reference measurement was chosen to be the first measurement after the devices were sealed because the aging characteristics before and after sealing differed radically. The computed variation was averaged over all the devices in each group and the standard deviation about this average was determined.

The best way to illustrate this processed data is through plots of the average change versus time. Figure 7 shows the variation of frequency with time. The plot contains both the oscillator data and the average of the 3-dB amplitude frequencies as measured on the spectrum analyzer. The length of the vertical bar is one standard deviation of the 20 data points. The tails on the ends of the bars extend to the left for spectrum analyzer data and to the right for oscillator data. It is clear that the data are in agreement. The analysis is based on an average of the two techniques to minimize the effects of systematic measurement errors.

In all cases, the frequency increases before the device is sealed and decreases shortly after sealing. The rate of change after sealing decreases with time which suggests a logarithmic dependence. The data are replotted on a logarithmic time scale in Figure 8. The approximately linear trend at large times is clear but the significance of the initial data is not. The frequency variation is analyzed further in Subsection I.E.

Figure 9 shows the variation of insertion loss with time. The data taken on devices aged at or below 100°C show a variation of ±0.5 dB over the 140-day measurement period. The initial insertion loss averaged 11.9 dB. At 150°C, the insertion loss appears to be increasing after 60 days, but the change is only 1 dB. At 200°C, the loss increased by 5 dB in the first 19 days and subsequently stabilized. During this period, 3 of the 20 devices failed completely and were dropped from the study group. No additional failures occurred. The loss for devices aged at 250°C showed similar behavior; a 10-dB increase in 19 days (with no device failures) and stable performance thereafter. Several failures occurred as testing continued at 250°C; four devices failed between 33 and 61 days, eight more between 61 and 89 days, and one between 89 and 117 days. No devices failed between 117 and 145 days. (The data taken after 117 days was taken after formal termination of the contract. Wherever possible this data has been added to this report, but it is missing in some of the figures. The devices are still on test.)

The behavior of insertion loss at temperature above 150°C is like that observed in the previous study where a different RTV was used. As described in reference 1, Subsection 4.D (page 4-29), this loss degradation can be traced to a deteriation of the gold-ball-bond to aluminum-bonding-pad interface. The current study shows that this interface can cause a significant degradation in performance at temperatures down to 150°C with the severity of the degradation increasing with temperature. The saturation observed at 200° and 250°C suggest a process that varies as

$$\Delta_{IL} = A\,[1 - \exp(-Bt)]$$

where Δ_{IL} is the change in insertion loss and A and B are temperature dependent constants. This effect was not observed below 150°C. The results indicate that the use of gold-ball-bond/aluminum interfaces should be avoided for devices exposed to temperatures in excess of 150°C. No significant changes in insertion loss were observed for the preaged or ZnO tuned devices.

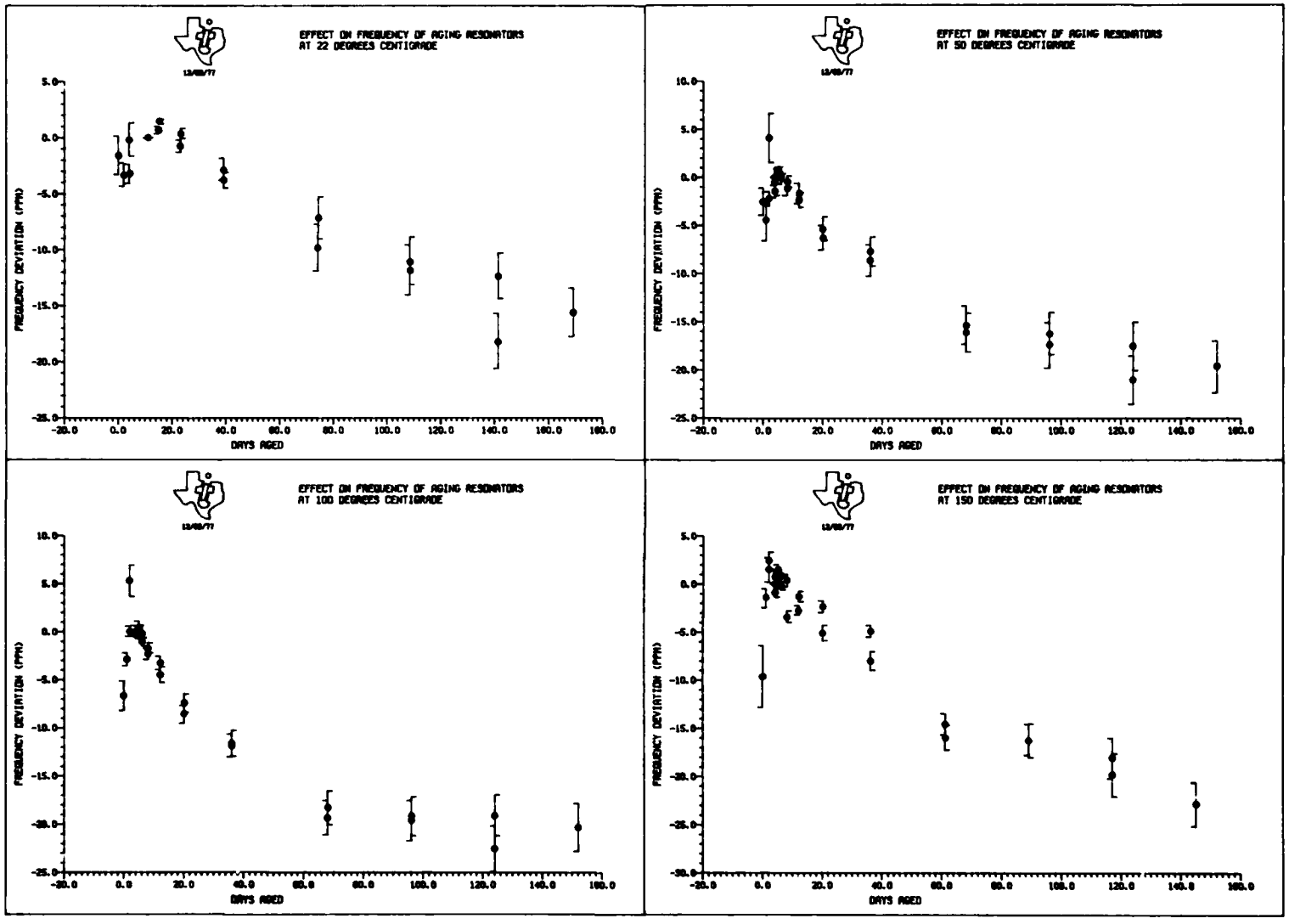

212605

Figure 7. Resonator Frequency Versus Aging Time (Sheet 1 of 2)

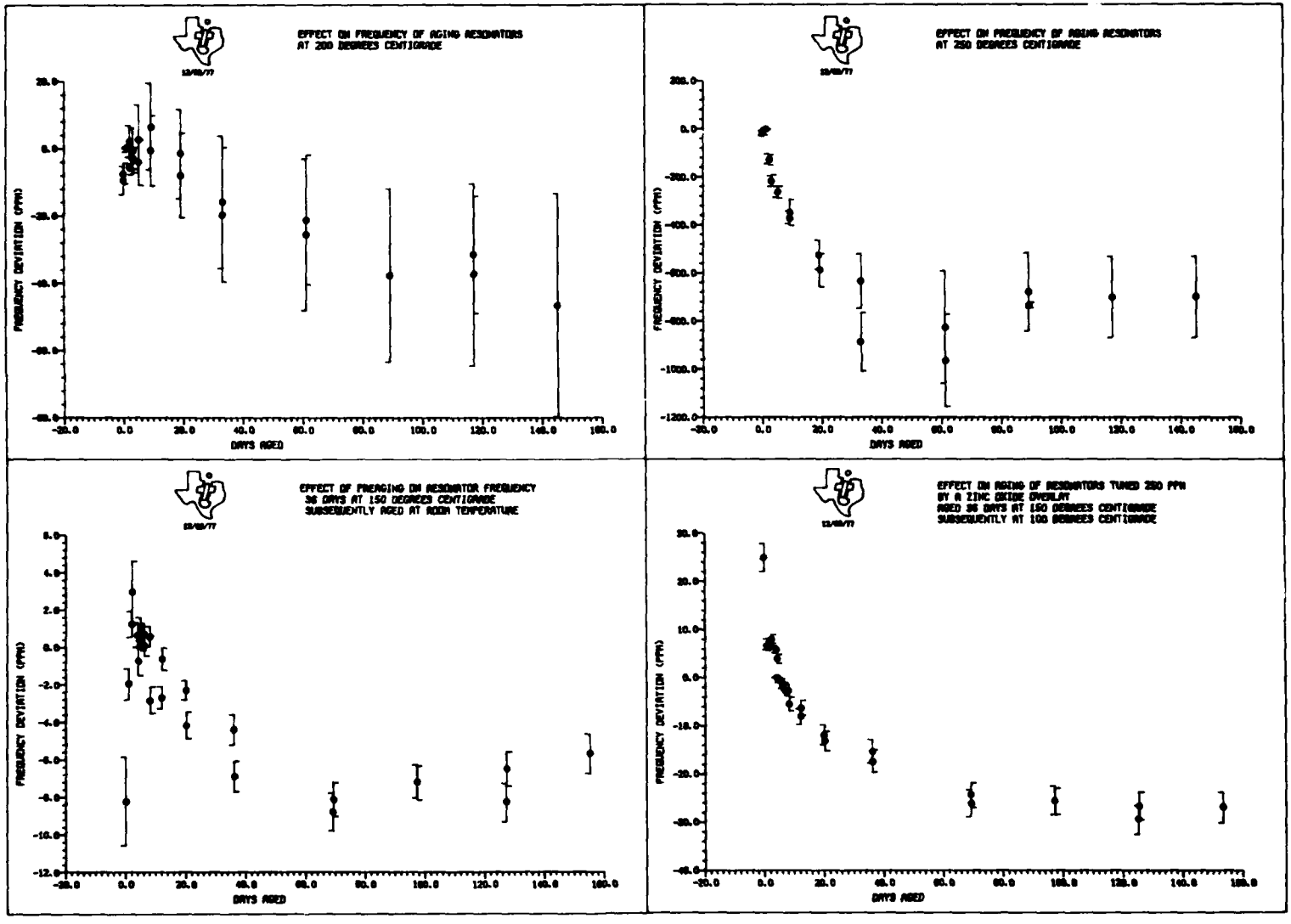

212604

Figure 7. Resonator Frequency Versus Aging Time (Sheet 2 of 2)

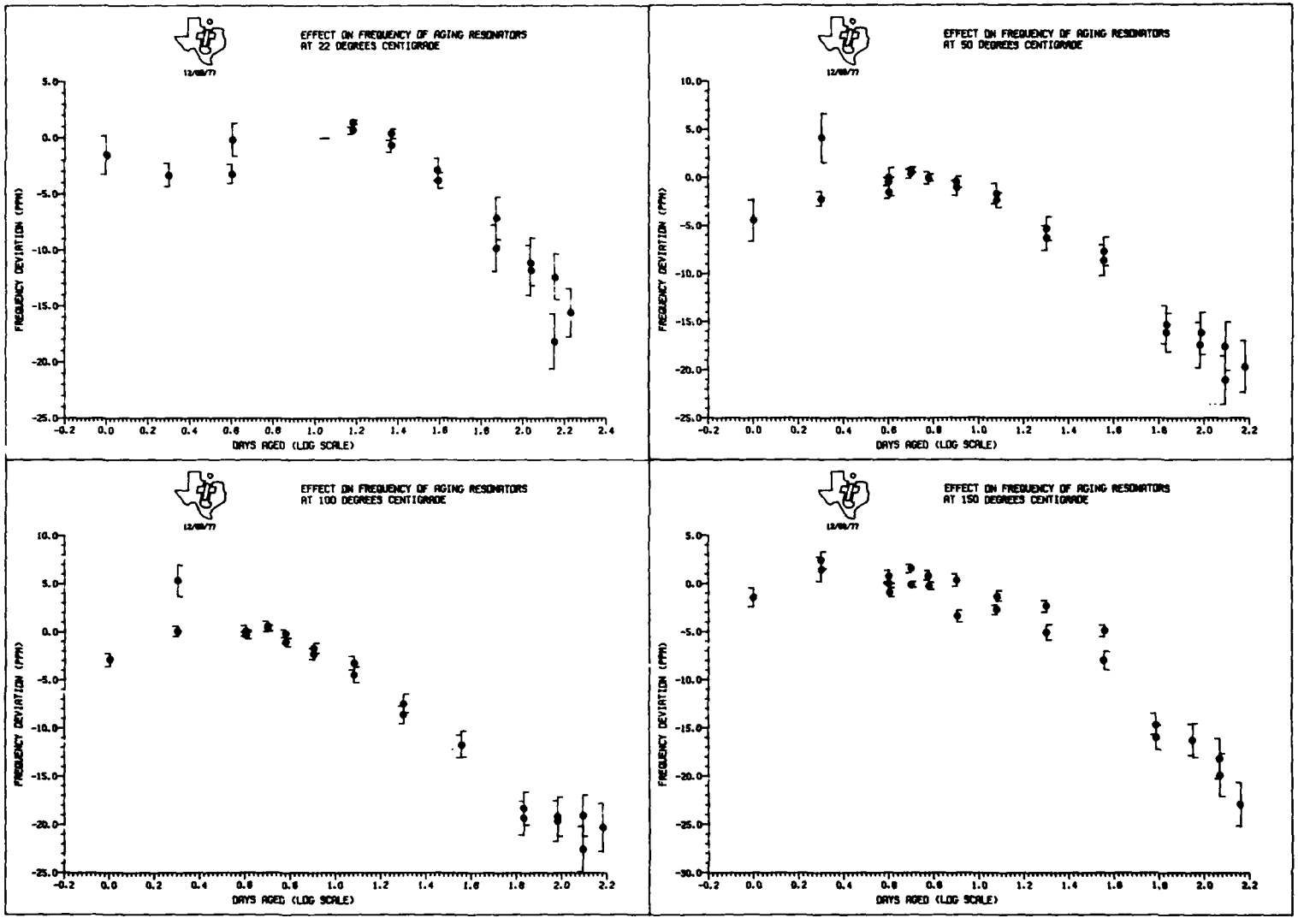

212603

Figure 8. Resonator Frequency Versus Logarithm of Aging Time (Sheet 1 of 2)

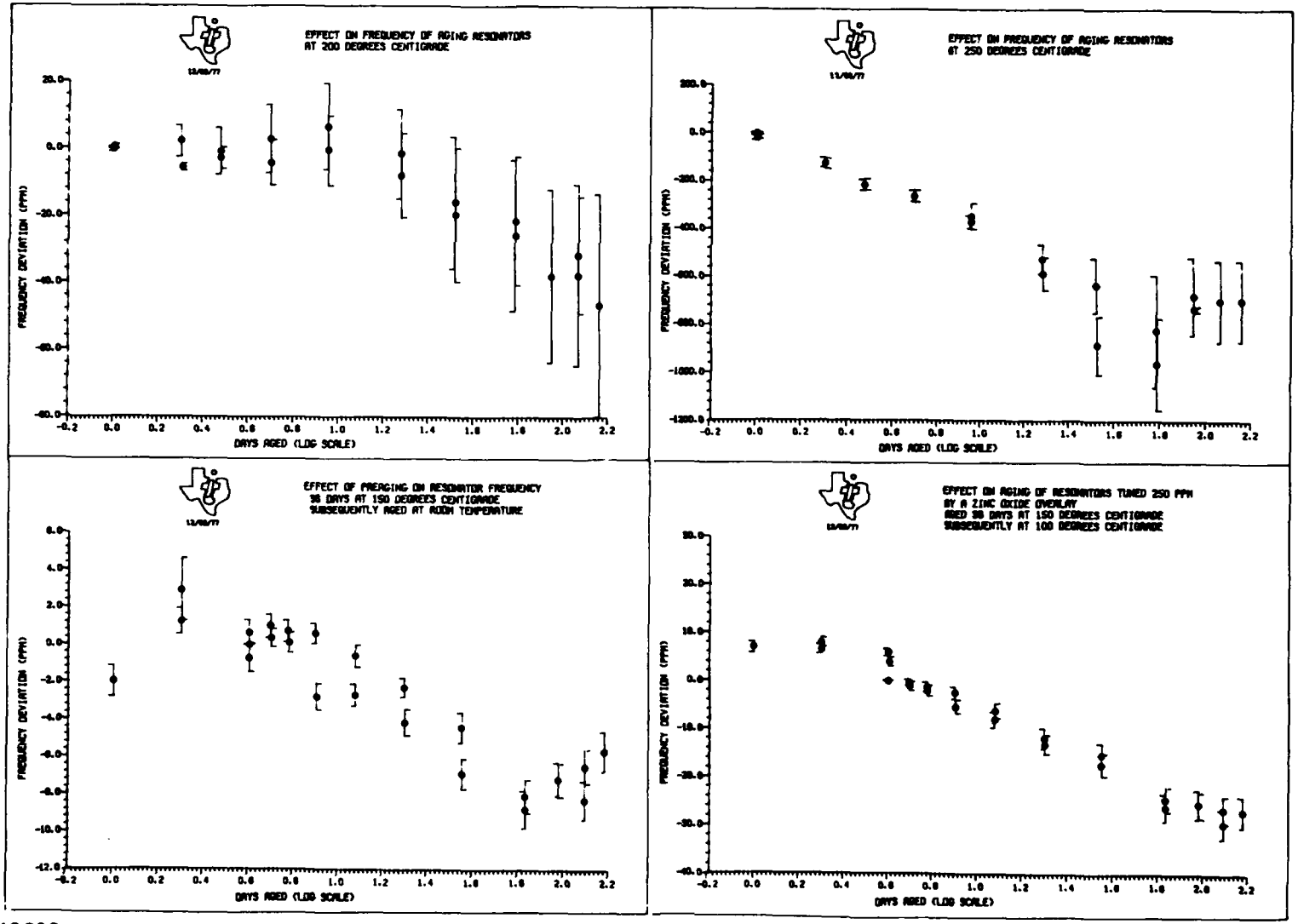

212606

Figure 8. Resonator Frequency Versus Logarithm of Aging Time (Sheet 2 of 2)

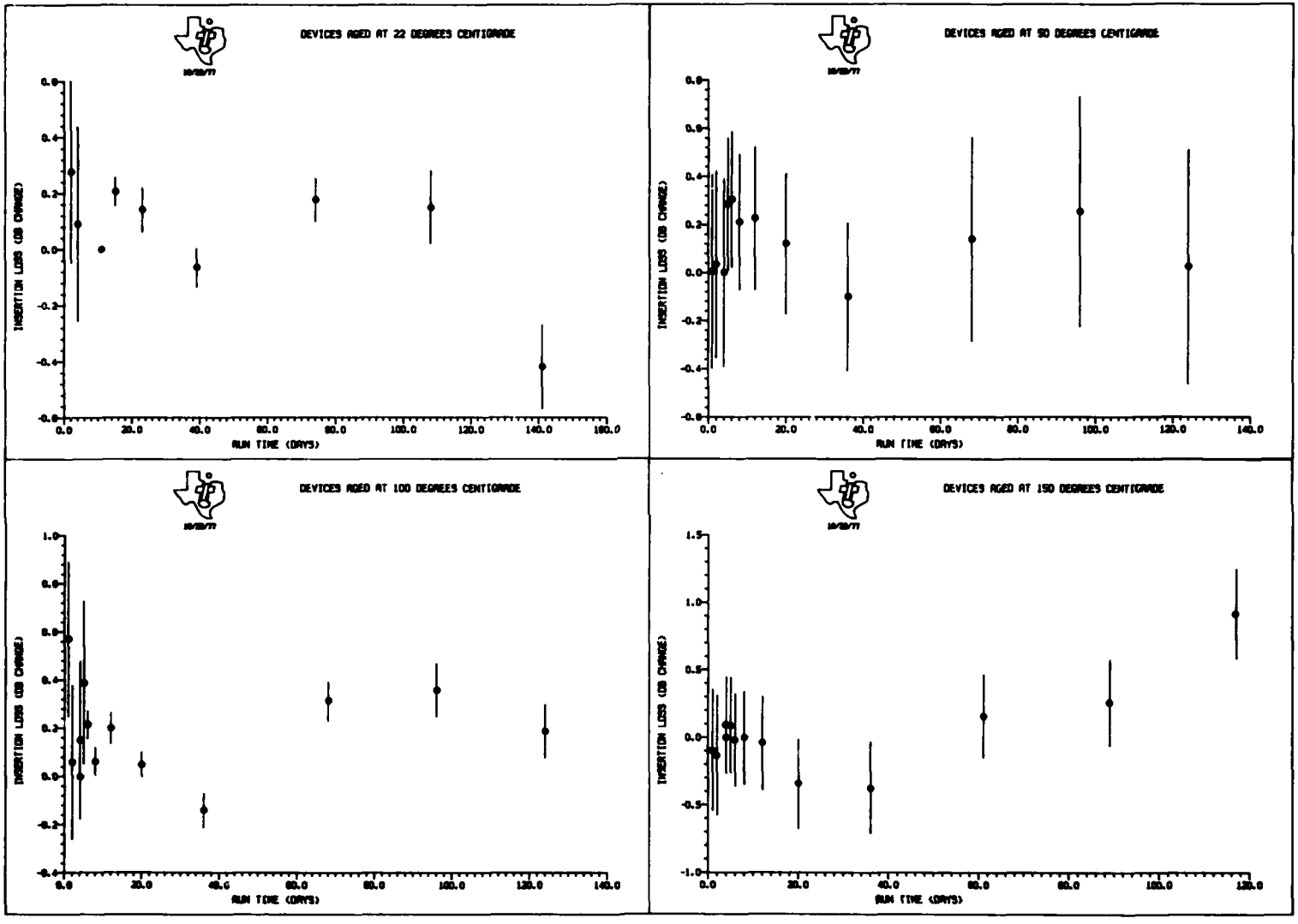

212607

Figure 9. Resonator Insertion Loss Versus Aging Time (Sheet 1 of 2)

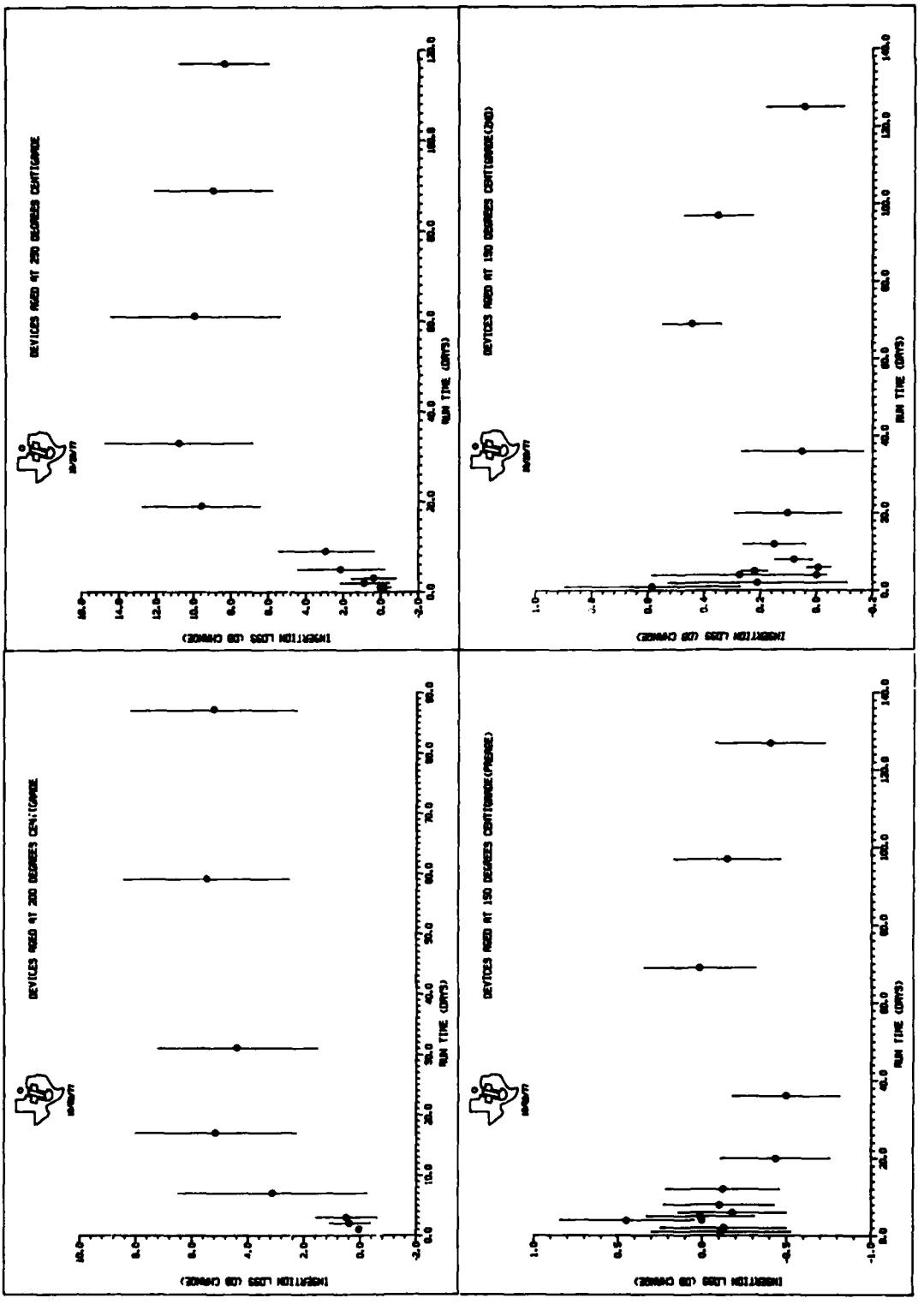

212608

Figure 9. Resonator Insertion Loss Versus Aging Time (Sheet 2 of 2)

The variation in the bandwidth of devices is shown in Figure 10. At 150°C and below, the bandwidth varies over a range of about 0.5 kHz. The initial bandwidth was 15.8 kHz at 194.41 MHz. At 150°C, a larger decrease, 1 kHz, is apparent after 117 days of aging. Large variations were observed on devices aged at 200° and 250°C. On the 200°C devices, the bandwidth decreased by 1 kHz, and on the 250°C devices, it increased by 3.5 kHz. These changes cannot be termed data trends since the standard deviation within these groups are 2.7 and 3.4 kHz, respectively. The preaged devices appear the same as the others aged at 150°C and below.

The ZnO tuned devices showed a slightly larger increase in bandwidth during the aging period at 150°C and a decrease when the temperature was reduced to 100°C. These changes may be related to an interaction of the ZnO and water vapor that was trapped in the can after sealing. This vapor could come from the walls of the can, the RTV, or the resonator itself. The reaction and equilibrium reached during aging would be different at the two aging temperatures.

The insertion loss (IL), bandwidth (BW), and resonant frequency (f_0) were combined to calculate the device unloaded Q. This relationship is as follows:

$$Q_u = \frac{f_o}{BW \times (1 - 10^{-IL/20})}$$

The results of this calculation are shown in Figure 11. As before, little variation is seen at temperatures of 150°C and below. The Q for these devices changed by only 400 from an initial value of 16,000 during the test period. The standard deviation of devices within each group was 300 to 400. At 200° and 250°C, the Q decreased further (by 1,100 and 5,000, respectively) but the spread of data within the groups also increased greatly. The standard deviations were 1,700 and 2,000. Therefore, although there is definitely more change at the higher temperatures, examination of the data on individual devices aged at 200°C shows that performance varies from no change in Q to a decrease of 5,000. Thus, individual device performance varies radically about the average. At 250°C, 13 devices failed during the testing. On the last measurement before failure, the change in Q varied from −500 to −15,000 so no real correlation can be drawn between the unloaded Q and the failure mechanism. On the remaining seven devices, the net decrease varied from 2,600 to 9,000.

The devices preaged at 150°C and subsequently aged at room temperature show no significant unloaded Q variation. The cumulative change was −170 with a standard deviation of 340. The devices tuned with ZnO showed a larger change but also a larger spread. The decrease in unloaded Q was 720 with a standard deviation of 420.

E. FREQUENCY DATA ANALYSIS

One goal of this program was to determine the dependence of aging on time to allow for extrapolation and to determine the dependence of aging on temperature. To achieve these ends, the data must be matched to a functional dependence. To arrive at a meaningful dependence, the data were fit to various functions and the parameters in those functions were varied to minimize the square of the difference between the predicted frequency and the measured frequency. The choice of function was based on minimizing this difference summed over all points (chi squared) per degree of freedom. The following functions were considered:

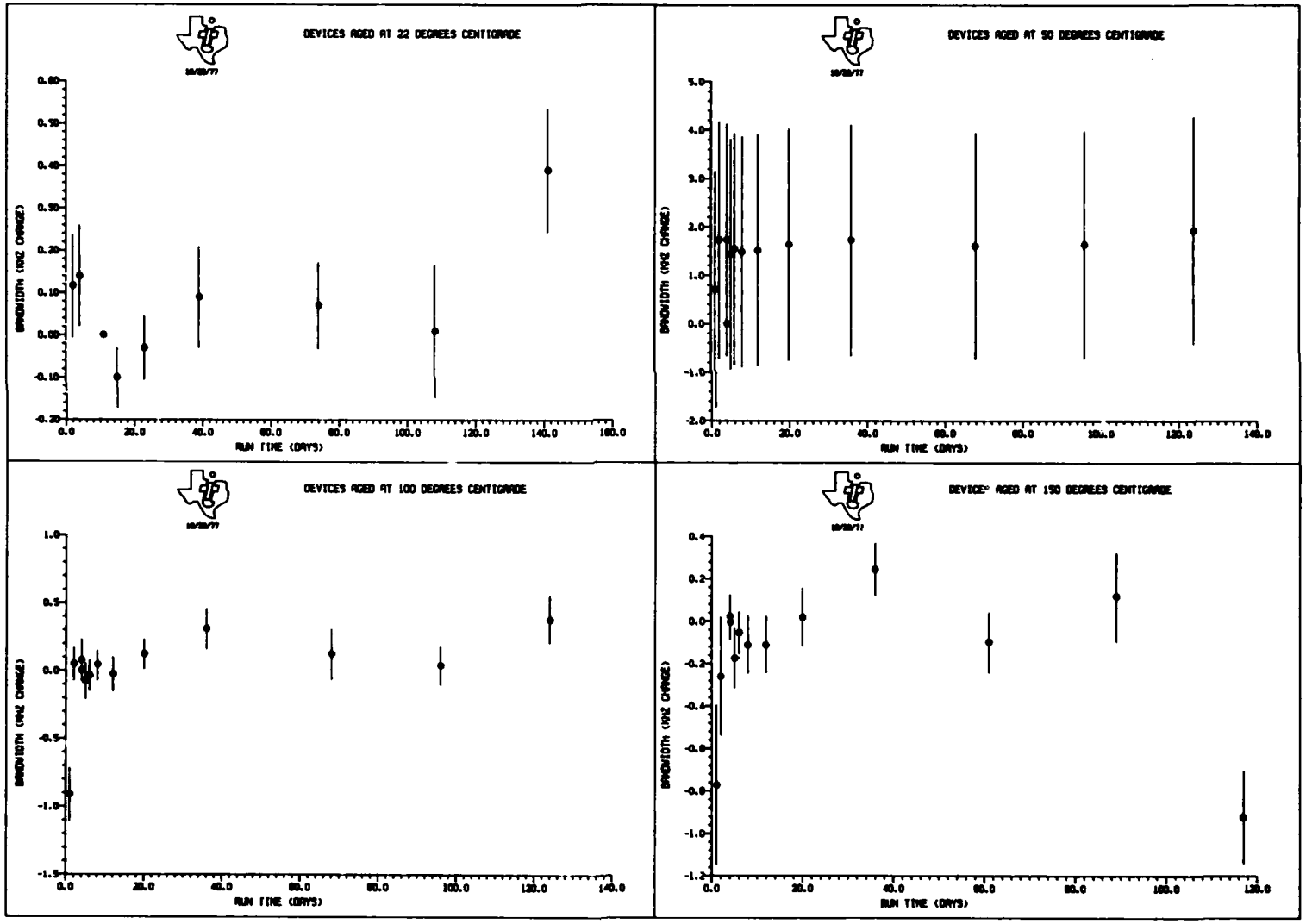

212609

Figure 10. Resonator Bandwidth Versus Aging Time (Sheet 1 of 2)

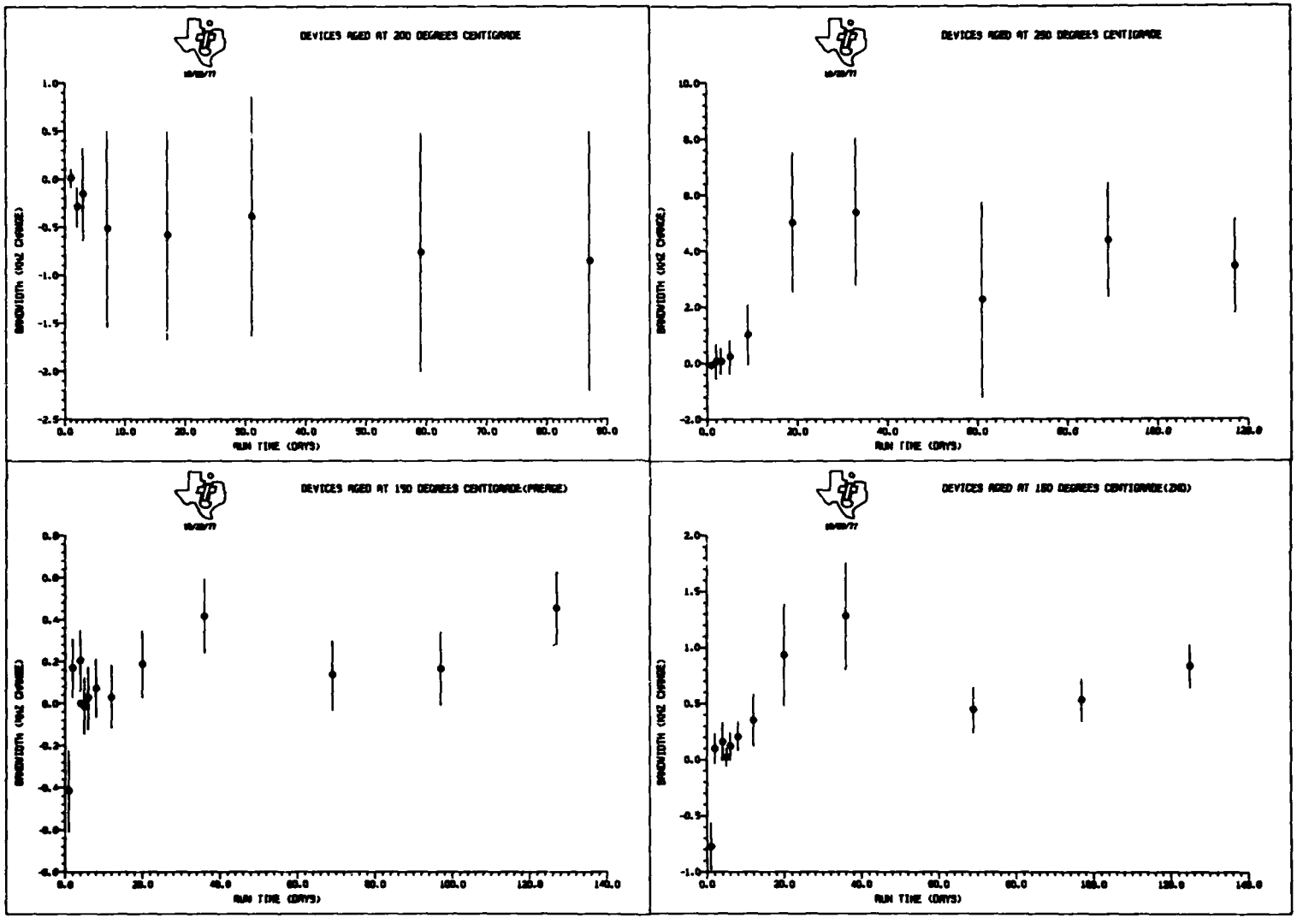

212610

Figure 10. Resonator Bandwidth Versus Aging Time (Sheet 2 of 2)

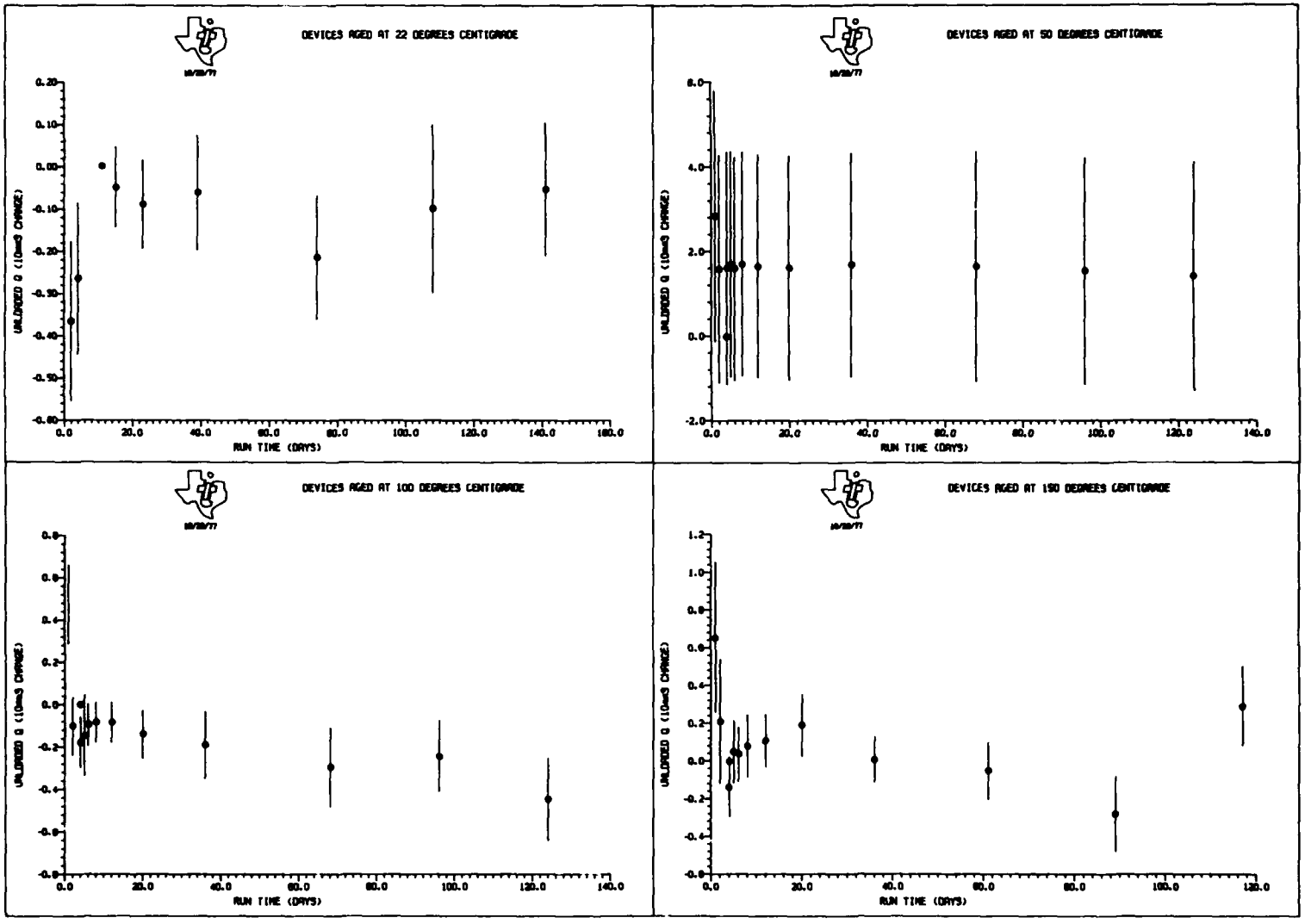

212612

Figure 11. Resonator Unloaded Q Versus Aging Time (Sheet 1 of 2)

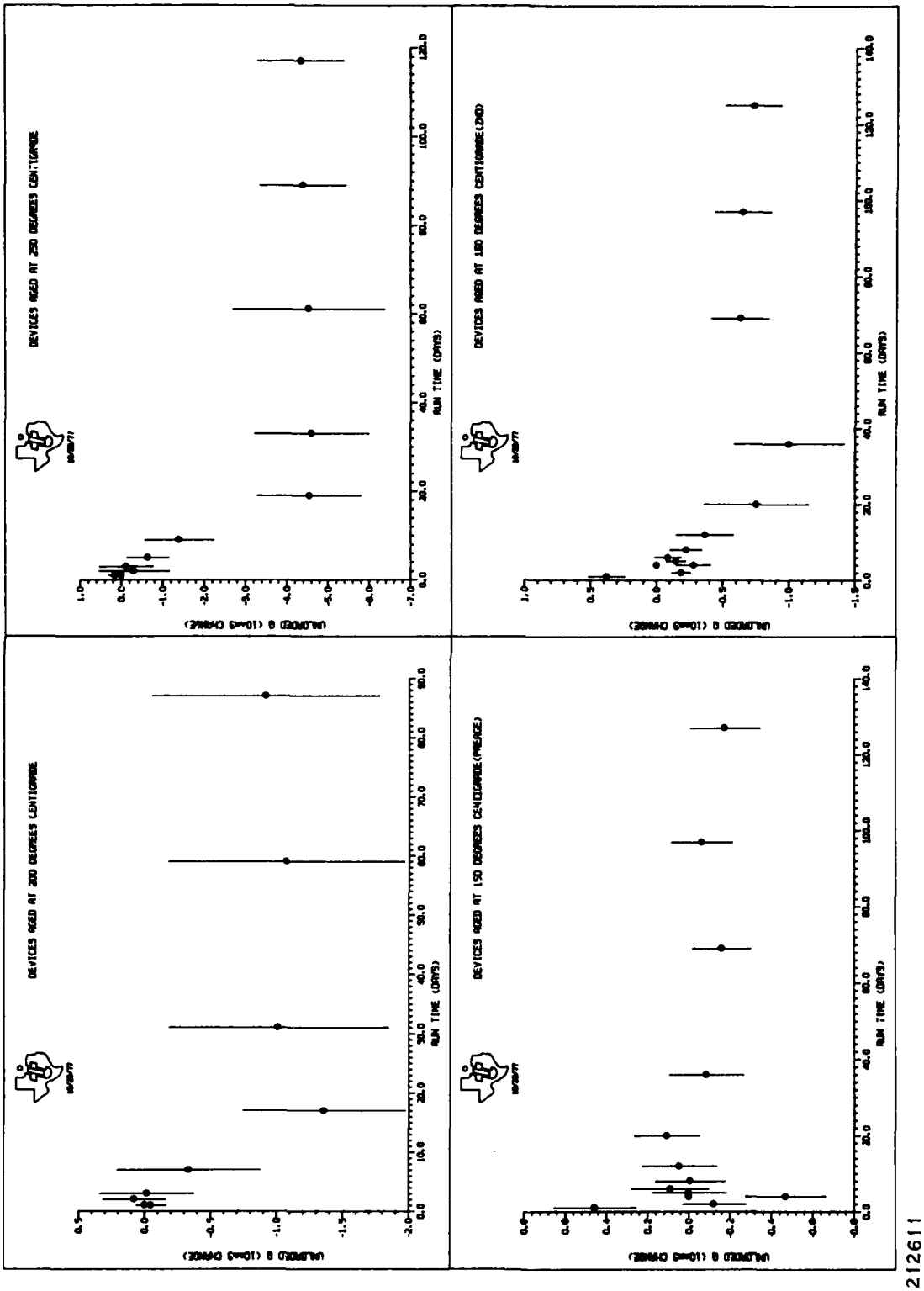

212611

Figure 11. Resonator Unloaded Q Versus Aging Time (Sheet 2 of 2)

$$y = A \log (1 + Bt) \tag{1}$$

$$\begin{aligned} y &= A \log (C + Bt) \\ &= A \log (1 + Bt/C) + A \log (C) \end{aligned} \tag{2}$$

$$y = A \log (1 + Bt) + C \log (1 + Dt) \tag{3}$$

$$y = A \log (1 + Bt) + C \log (1 + Dt) + E \tag{4}$$

$$y = A \log (1 + Bt) + C [1 - \exp (Dt)] \tag{5}$$

The first function represents a logarithmic process with an adjustable time reference and rate. The function is constrained to vanish at t = 0. The second function is the same as the first with the constraint removed. The third represents two logarithmic functions both constrained to vanish at t = 0. The fourth removes the contraint. The fifth function represents two processes, one logarithmic and one exponential. Both functions vanish at t = 0.

Examination of the data in Figure 8 shows radically different behavior before and after sealing. Since the period of interest is the time after sealing, the first data point after sealing (used as a reference in the plots) was defined as t = 0 in the functions and only the data taken after sealing were used in the analysis.

The procedure for obtaining a least squares fit to this data is given by Bevington.[3] For this analysis, the standard deviations were ignored since the deviation itself is defined as zero for the reference point. This definition creates an artificially low standard deviation for the early data. The method used here places an equal weight on all data points as opposed to emphasizing those with small standard deviations. With this method, the best fit (minimum chi-squared per degree of freedom) was obtained with functions (3) and (5). The major differences between these functions occur for small values of t. Function (3) reduces to two competing logarithmic processes for small t and the dependence at large t is dependent on both processes. The parameters in this function are not completely independent, which led to a slow convergence of the curve fitting routine and parameter values that vary greatly with small data changes.

Function (5) reduces to an exponential process that dominates the aging for small t and a logarithmic process that dominates for large t. Thus, the parameters are more independent, leading to more stable convergence. The exponential process models the initial rise after sealing that is noticeable in the low temperature data. Its effect dies away quickly. The logarithmic process models the decrease in frequency that begins a few days after sealing. In the high temperature data, the initial rise dies away so quickly that it can be modeled equally well in a statistical sense by function (2). In this case, the exponential in function (5) dies away completely between the first two data points; the parameter D merely allows the function to go through 0 at t = 0. In all cases the most sensible fit was judged to come from function (5). It was used on all of the data.

The resultant parameters from this fitting procedure are shown in Table 1. The table shows the parameters obtained for each group of devices. The columns on the right show the

[3] P.R. Bevington, *Data Reduction and Error Analysis for the Physical Sciences*, McGraw-Hill Book Co., (New York, 1969).

TABLE 1. DATA FIT TO A LOG $(1 + Bt) + C \cdot (1 - e^{Dt})$

Aging Temperature (°C)	Fitting Parameters A (ppm)	B ($days^{-1}$)	C (ppm)	D ($days^{-1}$)	Days Aged	Maximum Measured Shift (ppm)
22	−25	0.032	3.4	−0.33	158	−16
50	−18	0.13	3.5	−0.42	148	−20
100	−15	0.50	6.0	−0.58	148	−21
150	−27	0.12	11.0	−0.10	141	−23
200	−54	0.89	18.0	−0.13	144	−46
250	−330	3.20	58.0	−10.0	144	−700
150	−10	0.11	0.97	−10.0	32	−5
↓ 22 (preaged)	−51	2.8×10^{-3}			119	−7.3
150 (tuned)	−19	0.28	2.0	−10.0	32	−16
↓ 100 (tuned, preaged)	-8.2×10^{5}	6.8×10^{-7}			117	−28

number of days of aging that formed the basis for the data fit and the measured cumulative change at that time. The logarithmic dependence shows little acceleration below 150°C and a rapid acceleration (large A) at 200 and 250°C. The exponential process shows a consistent increase (increasing C) as the temperature rises. For the preaging and ZnO results at 150°C, there is insufficient data to obtain a good fit. The large negative value of D in both cases reduces the effect of the exponential process to that of a fixed offset after the first point. Thus, the logarithmic process is sufficient to model the frequency variation of the 32-day preaging cycle. After preaging, the additional data were again fit to the logarithmic process alone [function (1)] since the exponential process has been carried to completion during preaging. After preaging, the 120-day test period corresponds to an essentially linear porition of the logarithmic curve. Thus, the curve fit to this portion yields a linear best fit. When B is small the following approximations are valid:

$$A \log (1 + Bt) \cong ABt/\ln 10$$

Thus, the curve fit obtained on the preaged devices is nearly equivalent to linear againg rate of 16 ppm per year. The logarithmic dependence shows up only at the end of the test period.

The ZnO results are similar to the preaged devices. Again, the exponential process reduces to a fixed offset after the first point. After preaging, the data follow a 90-ppm per year variation. This rate of aging is faster than the −36-ppm per year measured on untuned devices that were left at 100°C for the same length of time that the ZnO devices were at 150°C. Thus, ZnO tuning degrades the aging performance of resonators significantly. This tuning method can be used only when a significant degradation in aging performance is tolerable.

The results of the curve fitting are shown in Figure 12 for a period of half a year (slightly more than the measurement time). These curves show some slight acceleration from room temperature to 150°C. These curves are extrapolated to 4 years in Figure 13. The similarity of results at or below 100°C is obvious. The results at and above 150°C show a strong acceleration with temperature. These extrapolated results must be viewed with caution since the trends are not entirely clear.

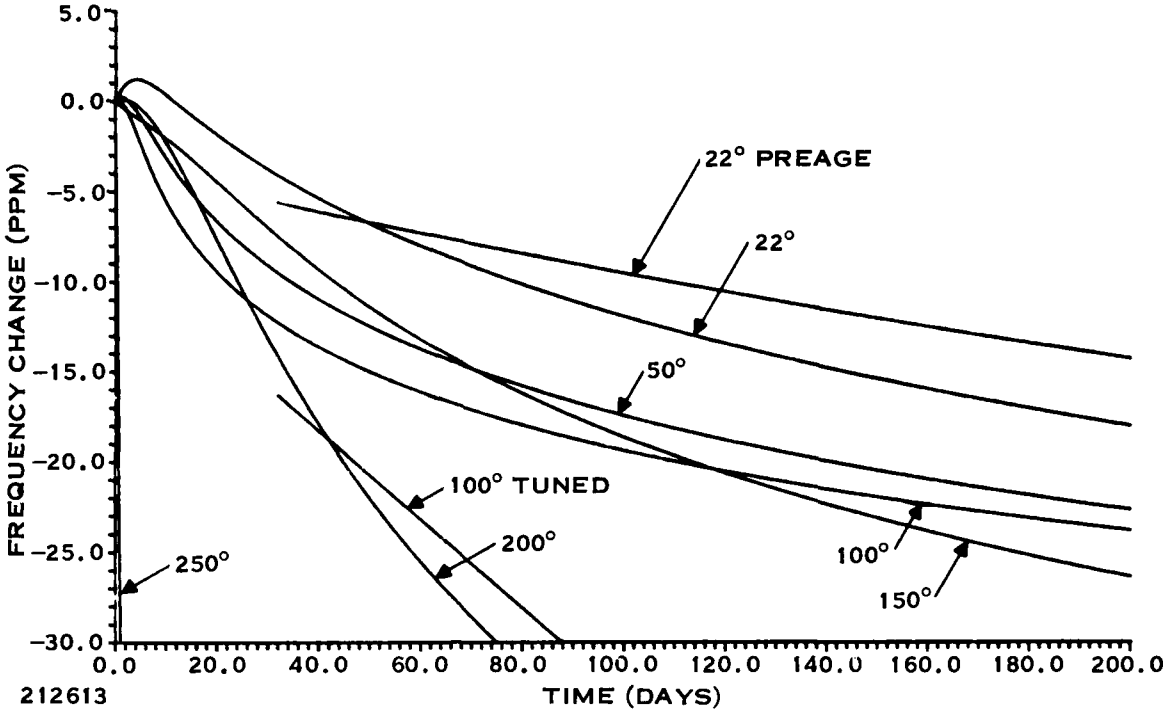

Figure 12. Effect on Frequency of Aging Resonators at 22°, 50°, 100°, 150°, 200°, and 250°C Least Squares Data Fit

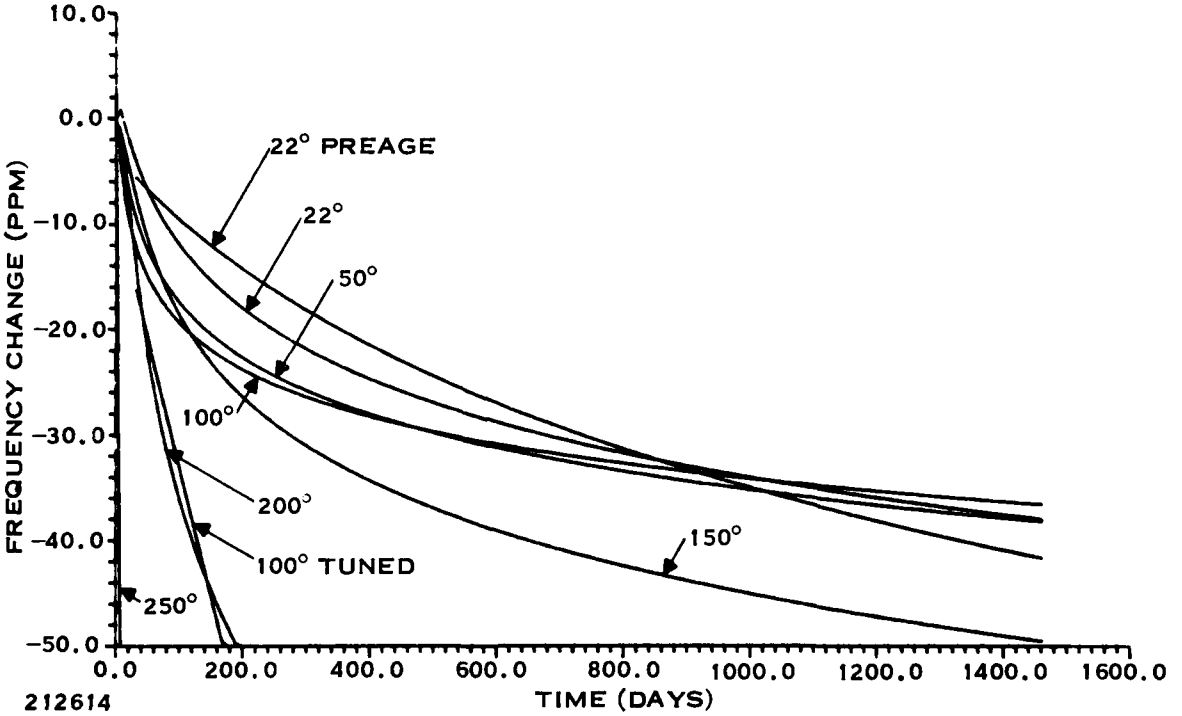

Figure 13. Effect on Frequency of Aging Resonators at 22°, 50°, 100°, 150°, 200°, and 250°C Extrapolation From Least Squares Data Fit

F. CONCLUSIONS

The aging study showed that current resonator fabrication and packaging leads to a device aging rate of 13 ppm per year in devices preaged for 4 months. A weak temperature dependence was observed at temperatures below 100°C. The extrapolated rates determined in this study indicate that after 6 months of preaging, rates below −10 ppm per year are possible at temperatures up to 100°C. From 150° to 250°C, this rate increases from −12 ppm per year to −157 ppm per year.

Other conclusions that can be drawn from this study are that operation above 150°C should be avoided and that a new tuning technique for grooved devices needs to be investigated. In addition, if lower aging rates are needed, new mounting techniques and packaging methods need to be found. In this area, much can be learned from precision bulk wave resonator production. The major deviations from those processes in this study were the RTV mounting material and sealing in a gold-plated package with a nitrogen atmosphere. Vacuum sealing needs investigation along with modern low leak rate packages.

SECTION II
HIGH-Q STUDIES

Achieving high Q is synonymous with identifying and reducing sources of loss in resonators. Therefore, the goal of this portion of the program is to identify the resonator design that results in the lowest loss characteristics. The highest Qs reported[4] have been obtained with reflectors consisting of arrays of grooves. These results, which approach the material Q of quartz and $LiNbO_3$, were obtained with no transducers in the cavity and large weighted arrays of shallow grooves. The goal of this work was to build a two-port resonator with both transducers inside the cavity that has an unloaded Q of 10^5 at 70 MHz. The approach used was to analyze the losses associated with two-port resonators currently being used, to translate these losses to 70 MHz, and to design a new device to achieve the high-Q goal. This approach led to the fabrication of a device with an unloaded Q of 40,000. The failure to reduce bulk wave scattering loss is explained and an improved approach is proposed. The devices built with this design were made into one-pole filters for delivery.

A. LOSS ANALYSIS

The loss in a resonator is measured by and is inversely proportional to its unloaded Q (Q_u). The Q_u is the limit of the loaded Q ($Q_L = f_o/\Delta f_{3\,dB}$) as the coupling to the cavity approaches zero. Losses in the resonator cavity ultimately limit this Q. To determine the relative importance of different loss mechanisms at different frequencies, it is convenient to define a separate Q for each loss. The net Q is then given by the sum of the losses or inverse Qs as stated in the following relation:

$$\frac{1}{Q_{net}} = \sum_i \frac{1}{Q_i}$$

where i covers all loss mechanisms. This approach has been used by Li, et al.,[4] and is discussed at length by Bell and Li.[5] The various loss mechanisms and their associated Q values at 70 MHz are listed in order of importance in Table 2. The basis for the data given in Table 2 follows.

1. Air Loading Loss

The major loss associated with the resonator at 70 MHz is air loading or radiation of energy into the surrounding atmosphere.[6] This effect limits the Q to 68,000. The value of the air loading Q, Q_a, was determined from measurements at 194.14 MHz of the difference in Q when a resonator was surrounded by air or vacuum. Q_a is equal to the ratio of the wave propagation constant β to twice the attenuation coefficient α_a. Since both β and α_a are proportional to frequency Q_a is independent of frequency. To achieve the design goal of 100,000 at 70 MHz, the device must be operated in vacuum.

[4] R.C.M. Li, J.A. Alusow, and R.C. Williamson, "Experimental Exploration of the Limits of Achievable Q of the Grooved Surface-Wave Resonator," *1975 Ultrasonics Symp. Proc.*, IEEE Pub. No. 75 CHO 994-4SU (September 1975), pp. 279–283.

[5] D.T. Bell, Jr., and R.C.M. Li, "Surface Acoustic Wave Resonators," *Proc. IEEE*, Vol. 64 (1976), p. 711.

[6] A.J. Slobodnik, Jr. "Attenuation of Microwave Acoustic Surface Waves Due to Gas Loading," *J. Appl. Phys.* 43:6 (1072), p. 2565.

TABLE 2. LOSS AND Q AT 70 MHZ

Loss Mechanism	Q	Source
Air loading	Q_a = 68,000	Measurements at Texas Instruments[7]
Viscous material	Q_m = 150,000	Szabo and Slobodnik[8]
Bulk scattering (unweighted array)	Q_b = 160,000	Alusow, et al.[9]
Transducer	Q_{IDT} = 700,000	Measurements at Texas Instruments
Reflection	Q_r = 1,500,000	Calculation
Surface scattering	Q_s = 3,400,000	Calculation based on Alusow[9]
Bulk scattering (weighted array)	Q_b' = 16,000,000	Calculation
Total in air	Q_u = 42,000	
Total in vacuum	Q_u = 110,000	

[7] W.R. Shreve, "Surface Wave Resonators and Their Use in Narrowband Filters," *1976 Ultrasonics Symp. Proc.*, IEEE Pub. No. 76 CH 1120-5SU (October 1976), pp. 706–713.

[8] T.L. Szabo and A.J. Slobodnik, Jr., "The Effect of Diffraction on the Design of Acoustic Surface Wave Devices," *IEEE Trans. Sonics Ultrason.* 3, (1973), p. 240.

[9] J.A. Alusow, R.C.M. Li, and R.C. Williamson, "Suppression of Bulk-Wave Scattering Loss in SAW Resonators," Paper P4, 1976 Ultrasonics Symp. (unpublished).

2. Viscous Material Loss

The ultimate limit of the Q is the viscous material loss represented by $Q_m = \beta/2\alpha$. Here α is the attenuation coefficient corresponding to viscous material losses, and it is a characteristic of the substrate. This coefficient is proportional to the square of the operating frequency,[10] so Q_m is inversely proportional to frequency. The limitation imposed by Q_m becomes more significant as the frequency increases. This effect accounts for the difference between the Q achieved with bulk resonators in the 10-MHz range and the Q achieved with SAW resonators in the 100-MHz range. At a given frequency, Q_m can only be changed by changing the substrate. The value of 150,000 in Table 1 is based on the value for vacuum attenuation at 1 GHz reported by Szabo and Slobodnik.[11]

3. Scattering Into Bulk Waves

In unweighted arrays, scattering of surface waves into bulk waves is a significant source of loss. The comparison between weighted and unweighted arrays performed by Alusow, Li, and Williamson[12] leads to a scattering Q of Q_b = 160,000 at 157 MHz. This value is independent of

[10] B.A. Auld, *Acoustic Fields and Waves in Solids*, Vol. II (John Wiley & Sons, New York, 1973), p. 298.

[11] T.L. Szabo and A.J. Slobodnik, Jr., op. cit.

[12] J.A. Alusow, R.C.M. Li, and R.C. Williamson, op. cit.

frequency, since it is a function of the geometry; scaling the geometry changes the energy stored and energy dissipated per cycle in the same manner. With no suppression of this scattering, the Q of the 70-MHz resonator would be limited to 77,000 by the material losses and bulk scattering losses. Therefore, array weighting is necessary.

The scattering of Rayleigh waves from the array into bulk waves was studied with an approach similar to that previously developed to analyze the excitation of plate modes by an interdigital transducer.[13] In this analysis, a frequency dependent array factor for scattering into a single mode is calculated by examining the scattering of Rayleigh waves into Rayleigh waves (i.e., reflection). This array factor is assumed to be constant for scattering into any mode. Therefore, a superposition of the array factors for all modes with the proper amplitude and phase adjustments to account for mode coupling differences should give the net scattering by the array as a function of frequency. Weighting the reflector array allows one to change the array factor and thereby minimize scattering into plate modes at the resonant frequency. This technique gave extremely accurate results for the frequency response of an interdigital transducer where the driving mechanism is charge on the transducer and is essentially uniform along the transducer.

In the reflection case, the only frequency of interest is the resonant frequency that is near the frequency of maximum reflection of the Rayleigh wave. At this frequency, the driving mechanism, the Rayleigh wave, decreases in amplitude as the distance into the array increases. This change in driving strength must be included in the analysis of resonator reflector scattering. The strength of the bulk wave excitation was determined from the maximum array factor sidelobe more than 4.5 percent away from the synchronous frequency. The lowest velocity of the family of slow quasi-shear plate modes on ST quartz is about 4.5 percent above the Rayleigh velocity. The fast quasi-shear and longitudinal modes begin at relative velocities of 1.61 and 1.82, respectively. Thus, all sidelobes more than 4.5 percent must be suppressed.

This approach has been used to predict the dependence of scattering on the array weighting profile. The results for different weighting functions are shown in Table 3. The weighting functions are illustrated in Figure 14. Several conclusions are apparent from the values in the table. The slope of the profile at the array edge should be small. This is demonstrated by the poor suppression found for $\sqrt[4]{x}$ and by the difference between 1 + cosine and Gaussian suppression. These two are significantly different only at the edge of the array. The number of reflectors weighted is important in the ultimate suppression. It will also affect the effective cavity size; weighting too many reflectors can lead to a cavity that supports multiple modes. An array with a weighting of 1 + cosine in 20 reflectors was chosen for the high-Q design.

The effects of changing the number of reflectors in the array and the depth of the grooves (reflection per stripe) were examined for 1 + cosine weighting. The effect on scattering suppression of varying the number of reflectors is slight. This can be seen from the results in Table 2 for 20 reflectors weighted in arrays of 400 and 600 reflectors. If the groove depth of the 400 reflector array is increased from 0.013 wavelengths to 0.020 wavelengths, its reflectivity becomes equal to that of a 600-element array, with 0.013 wavelength deep grooves. This depth change only reduces the bulk scattering suppression from 25 dB to 21 dB. Implementation of

[13]R.S. Wagers, "Plate Mode Coupling in Acoustic Surface Wave Devices," *IEEE Trans. Sonics Ultrasonics*, **SU-23** (1976), p. 113.

TABLE 3. BULK SCATTERING SUPPRESSION

Weighting Profile	Reflectors Weighted/Total	Groove Depth (h/λ)	Suppression (dB)
Unweighted	0/600	0.013	Reference
1 + cosine	10/600	0.013	4
1 + cosine	20/600	0.013	25
1 + cosine	40/600	0.013	30
1 + cosine	80/600	0.013	38
1 + cosine	20/400	0.013	25
1 + cosine	20/400	0.020	21
Gaussian	10/600	0.013	5
Gaussian	20/600	0.013	18
Gaussian	40/600	0.013	26
Gaussian	80/600	0.013	26
$\sqrt[4]{x}$	10/600	0.013	5
$\sqrt[4]{x}$	20/600	0.013	5
$\sqrt[4]{x}$	40/600	0.013	7
$\sqrt[4]{x}$	80/600	0.013	9
Sine	10/600	0.013	5
Sine	20/600	0.013	15
Sine	40/600	0.013	20
Sine	80/600	0.013	26

weighting with suppression of 20 to 25 dB reduces bulk scattering loss by a factor of 100 to 300. As shown in Table 2, suppression increase Q_b to more than $1.6 \times 10.^7$ Scattering at this point has a negligible effect on the total device Q. Therefore, this design with 400 grooves 0.020 wavelengths deep was chosen for the test devices.

4. Transducer Loss

The transducers in the resonator cavity represent an additional source of loss. The loss consists of ohmic loss caused by transducer parasitic resistance and of viscous loss in the metal film. The combined effect has been calculated from measurements at 194 MHz. The measurements made by Alusow, et al.,[14] were used to characterize cavity losses (surface scattering losses, Subsection II.A.6) with no transducers in the cavity. If one assumes that all losses not associated with the transducer are included in Table 2, then calculated Q values at 194 MHz can be combined with the measured Q to obtain a value for the transducer Q, Q_{IDT}. This procedure yields a value of 250,000 for Q_{IDT}. The viscous metal loss has the same 1/f dependence on

[14]J.A. Alusow, R.C.M. Li, and R.C. Williamson, op. cit.

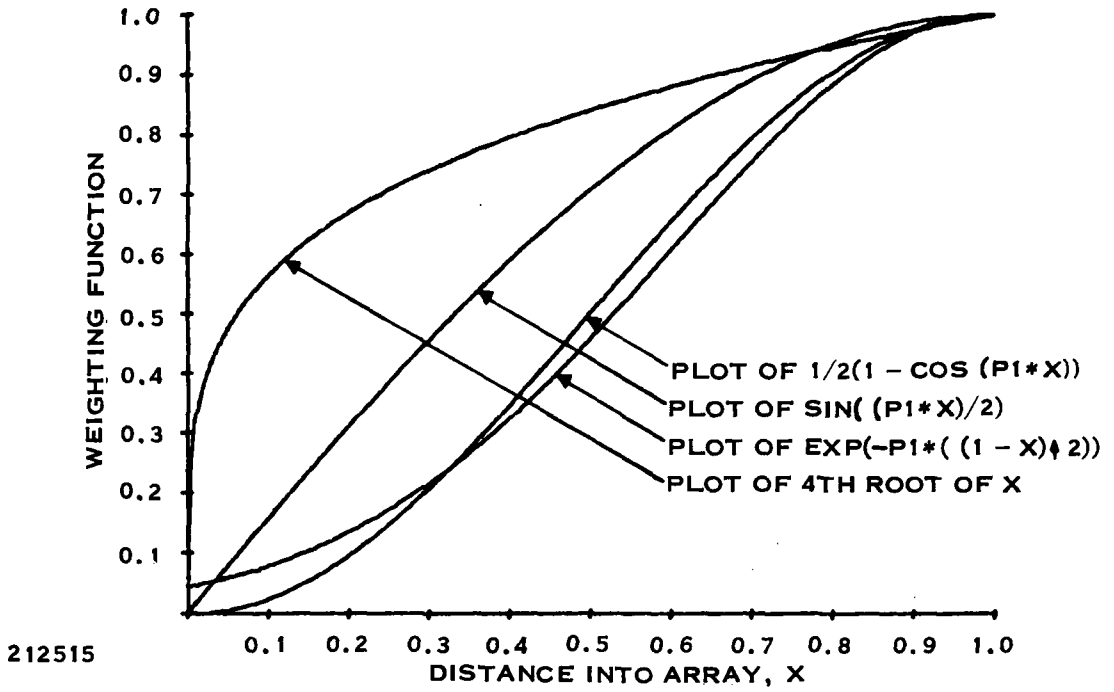

Figure 14. Array Weighting Functions for Suppression of Scattering Into Bulk Waves

frequency as the viscuous material loss discussed earlier. The Q corresponding to parasitic ohmic loss can be shown to depend solely on the transducer thickness. If this thickness is scaled inversely with frequency in the same manner that the rest of the resonator geometry is scaled, the total transducer Q is inversely proportional to frequency. This assumption gives the value Q_{IDT} = 700,000 at 70 MHz.

5. Reflection Loss

The reflection Q is fixed by the reflection coefficient of the arrays, Γ;

$$Q_r = 2n\pi/(1 - \Gamma^2)$$

where the effective cavity length is $n\lambda$. The reflection coefficient was evaluated using a standard lossless equivalent circuit representation for the reflectors modified to account for the weighting used for bulk scattering suppression. The result was Γ = 0.9999 corresponding to $Q_r = 1.5 \times 10^6$.

6. Surface Scattering

With no transducers in the cavity and bulk scattering suppressed, Alusow, Li, and Williamson still had loss in addition to the viscous material loss. This loss was the result of either

incomplete bulk scattering suppression, since the weighting profile was uncontrolled, or surface scattering. If it were all due to surface scattering (i.e., propagation loss caused by surface roughness), the Q at 157 MHz would be 1.5×10^6. It has been shown theoretically that this loss can be modeled as a uniformly distributed viscous loss.[15] Therefore, the associated Q should vary as Q_m. The contribution of surface scattering at 70 MHz becomes $Q_s = 3.4 \times 10^6$.

B. HIGH-Q RESONATOR DESIGN

The conclusion of this analysis is that a resonator can be built at 70 MHz with an unloaded Q in vacuum in excess of 10^5. The design must include bulk mode scattering suppression, a high reflectivity grating, and appropriately designed transducers. The theoretical losses for this design are shown in Table 1.

A two-port resonator was designed to verify the analysis. Each transducer had 20 split finger pairs, and each grating had 400 reflectors designed for a groove depth of $h/\lambda = 0.020$. Twenty reflectors at the edge of each array were weighted by a "1 + cosine" weighting function.

Many techniques have been demonstrated for weighting interdigital transducers and most are applicable for weighting resonator reflectors. The major criteria for choosing a weighting method are that the phase under the array is not distorted, that the technique introduces no new losses, and that the beam profile remains undistorted and therefore coupling between the fundamental mode and unwanted transverse modes is not introduced.

Groove depth weighting has been successfully demonstrated,[16] but problems have been reported with maintaining the depth uniformity across a groove. This nonuniformity distorts both the amplitude and phase of the wave and thereby couples energy into unwanted transverse modes.

Another technique that has been used on resonators to suppress bulk scattering is to use very shallow grooves.[17] This technique requires long gratings to achieve sufficiently high reflectivity. At 310 MHz, 1,000 reflectors were required in each array. To maintain the same bulk-Q/material-Q ratio at 70 MHz, a shallower groove would be required since the material Q is four times as large. If $Q_b \propto (h/\lambda)^{-3}$, then 1,640 reflectors would be required. The device would be more than 7.4 centimeters (2.9 inches) long. Clearly, some weighting technique is desirable at this frequency.

Withdrawal weighting has been used successfully on interdigital transducers but is not appropriate here. This type of weighting would result in sections of the reflector being undersampled; sections would have a periodicity corresponding to a higher fundamental frequency. In these sections, bulk waves would be efficiently coupled to Rayleigh waves and, therefore, bulk scattering loss would be large. This effect corresponds to high far-out sidelobes when interdigital transducers are withdrawal weighted. These sidelobes are suppressed by matching networks and cause no problems. The bulk scattering cannot be suppressed in a withdrawal weighted reflector.

[15]B.A. Auld, *Acoustic Fields and Waves in Solids*, Vol. II, John Wiley & Sons (New York, 1973), p. 311.

[16]R.C.M. Li, J.A. Alusow, and R.C. Williamson, op. cit.

[17]R.C.M. Li, "310-MHz SAW Resonator With Q at the Material Limit," *Appl. Phys. Letters*, Vol. 31:7 (1977), p. 407.

The reflection coefficient of a single groove can also be altered by varying its width. This requires precise lithographic control of line width, a difficult specification. In addition, the precise dependence of reflection coefficient on line width has not been extensively studied. It involves the application of a theory for reflection that includes stored energy over a large range of frequencies. To date, stored energy theory[18] has been confined to narrowband, near resonance approximation. Therefore, this technique was not used.

Apodization (varying the length of a reflector to control its reflectivity) can be used at the end of the array away from the cavity, but it introduces an unacceptable phase distortion across the width when used on the cavity end. Dot array weighting[19] is similar to apodization in that the reflector is weighted by replacing the solid line by a series of dots. Since the gaps are distributed across the beam, only small local phase distortions are introduced. The average effect over many reflectors is negligible.

A reflector segmentation technique between apodization and dot weighting was used in this program. Each weighted reflector was divided into 10 segments that were evenly spaced across the width of the array. The position of each section was randomized with respect to the position of sections of other weighted reflectors to reduce phase distortion and excitation of unwanted waveguide modes. As mentioned previously, the first 20 reflectors in each array were weighted with a 1 + cosine weighting function.

Two types of transducers were used on these resonators. The first was a conventional split finger transducer with cosine apodization to suppress transverse modes. The second was a jogged design intended to suppress the direct transmission between transducers. This design has been used previously within Texas Instruments, but this is the first time it has been discussed outside the company. With the direct transmission suppressed, the out-of-band rejection is limited only by the reflection sidelobes of the array. A schematic of this type of resonator is shown in Figure 15. The electrodes of each transducer have a 90-degree jog in the center. These jogs are in

[18]R.C.M. Li and J. Melngailis, "The Influence of Stored Energy at Step Discontinuities on the Behavior of Surface-Wave Gratings," *IEEE. Trans. Sonics Ultrasonics*, **SU-22**:3 (May 1975), pp. 189–198.

[19]L.T. Soli, "Surface Acoustic Ray Reflective Dot Array (RDA)," *Applied Physics Letters*, **28**:8 (April, 1976), pp. 420–422.

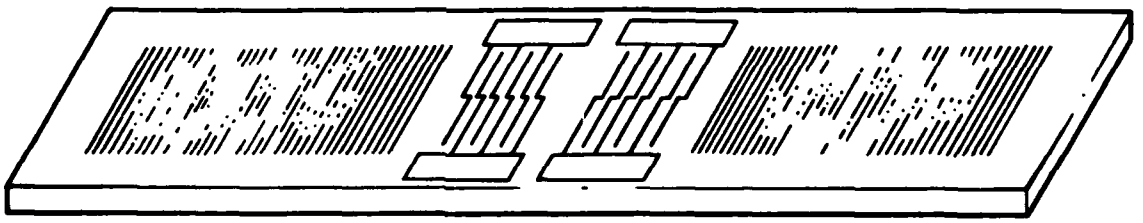

212516

Figure 15. Resonator Schematic (Jogged transducers improve out-of-band response)

opposite directions so the direct transmitted signals received on the two sides of the receiving transducer are 180 degrees out of phase; therefore, they cancel. The resonant standing wave position is determined by the reflectors alone; the jog in the transducers has no effect on the standing wave position. The only effect of the jog is to reduce the coupling at resonance by a factor of $\sqrt{2}$. This reduction is a result of the fact that the jogged transducer fingers cannot rest on the straight crest of the standing wave.

C. EXPERIMENTAL RESULTS.

Devices were fabricated with 0.013-wavelength-deep and 0.020-wavelength-deep grooves. The expected unloaded Qs of these devices were 29,600 and 42,000 respectively in air and 52,500 and 109,000 when measured in vacuum. Actual measured devices exhibited lower Q and contained a design error that resulted in two strong modes in the resonator cavity. These two problems are discussed in more detail below. Due to a lack of time and funds in the current program, a redesign was not performed. The devices were built into filters as described below for delivery to the contracting agency.

1. Q Measurements

Eleven devices were tested in this program. Five had conventional transducers and six had jogged transducers. Three of the 11 were built with 0.013-wavelength-deep grooves and the remaining eight had 0.020-wavelength-deep grooves. The results are shown in Tables 4 and 5. The shallow groove devices showed the highest Q ranging from 17,800 to 26,400. The device with the low Q had a scratch on one transducer that could account for the excessive loss. The Q of the deep groove devices varied from 17,800 to 22,500. These values are significantly less than the expected values. The two highest Q devices were measured in vacuum. As shown in Table 4, the Q increased to 37,500 and 39,600 for the two devices.

If no bulk scattering suppression were achieved by the weighting technique, these results are understandable. With no suppression, bulk scattering is inversely proportional to the groove depth cubed. Thus the bulk scattering is larger for the deep groove reflectors. When this decrease in Q_b and the increase in Q_r are both considered, the theoretical Q in air without bulk scattering suppression becomes 25,000 for shallow-groove devices and 21,500 for deep-groove devices. This agrees with the measured results. Similar agreement is obtained for calculations corresponding to the vacuum measurements. These comparisons are presented in detail in Table 6.

These results show that the segmented reflector weighting is not effective in suppressing bulk scattering. The reason for this result is clear if one views the wide reflector as many adjacent narrow reflectors. Each narrow reflector is withdrawal weighted and therefore each scatters coherently into some plate modes. The discussion in Subsection II.B. on withdrawal weighting is applicable here. Thus, the array will scatter into plate modes and the weighting will not be effective in suppressing bulk scattering loss.

2. Jogged Transducers

The use of jogged transducers to suppress direct transmission between transducers in resonator filters has been shown to be effective. Figure 16(A) shows the transmission between transducers jogged in the same direction. This no-suppression case has a loss of 40 dB. When the

TABLE 4. MEASUREMENTS ON RESONATORS WITH 0.013-WAVELENGTH-DEEP GROOVES

Device Number	f_o (MHz)	BW (KHz)	Loss (dB)	$\frac{Q_u}{1000}$	IDT Type	Measurement Conditions
4	70.1615	3.1	16.8	26.4	Conventional	In air
5	70.1522	3.6	14.6	23.9	Jogged	In air
6	70.1515	4.6	17.0	17.8	Jogged	In air
4	70.1615	2.2	14.2	39.6	Conventional	In vacuum
5	70.1522	2.5	12.0	37.5	Jogged	In vacuum

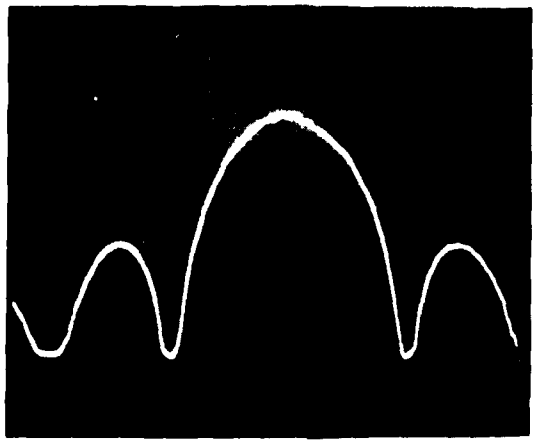

Figure 16. Jogged Transducer Delay Line Frequency Response

TABLE 5. MEASUREMENTS IN AIR ON RESONATORS WITH 0.020 WAVELENGTH-DEEP GROOVES

Device Number	f_o (MHz)	BW (KHz)	Loss (dB)	$\frac{Q_u}{1000}$	IDT Type
8	70.0853	3.8	14.8	22.5	Jogged
3	70.0850	4.1	13.4	21.7	Jogged
1	70.0818	4.4	12.0	21.3	Conventional
9	70.0727	4.0	15.9	20.9	Jogged
7	70.0809	4.4	12.8	20.7	Conventional
2	70.0664	4.2	17.2	19.4	Conventional
11	70.0675	4.5	14.1	19.4	Conventional
10	70.0720	4.6	16.7	17.8	Jogged

TABLE 6. COMPARISON OF EXPERIMENTAL AND THEORETICAL

Groove Depth (wavelengths)	$\frac{Q_r}{1000}$	$\frac{Q_b}{1000}$	Theoretical $Q_u/1000$	Experimental $Q_u/1000$	Measurement Conditions
0.013	97	16,000*	30	18 to 26	In air
0.013	97	160**	25	18 to 26	In air
0.013	97	16,000*	53	38 to 40	In vacuum
0.013	97	160**	40	38 to 40	In vacuum
0.020	2,800	14,000*	42	18 to 23	In air
0.020	2,800	44**	22	18 to 23	In air

* With bulk scattering suppression
** Without bulk scattering suppression

measurement is made between transducers jogged in opposite directions, the response is suppressed as shown in Figure 16(B). The loss is 62 dB, more than 20 dB down from the unsuppressed case.

The effect on out-of-band rejection when the jogged technique is used in resonators is shown in Figure 17. Figure 17(A) shows the frequency response of a resonator made with conventional transducers. This contains little information about the reflector stopband. Figure 17(B) shows the response of a similar device with jogged transducers and 0.013-wavelength-deep grooves. The 8- to 20-dB improvement in out-of-band response is clear. The direct transmission has been suppressed. The remaining sidelobes correspond to sidelobes of the reflection coefficient.

The effect of groove depth on reflection coefficient sidelobes close to the peak can be observed in the devices with jogged transducers. Figure 17(C) shows the response of a resonator with jogged transducers and 0.020-wavelength-deep grooves. The reflection coefficient sidelobes have increased by from 6 to 8 dB from those in Figure 17(B). The weighting chosen for this study was designed to reduce far out sidelobes. More weighting is necessary to reduce these close in sidelobes, but this weighting can be implemented on the outside and of the array to reduce problems with phase distortion. Straightforward apodization should be adequate. The effects of

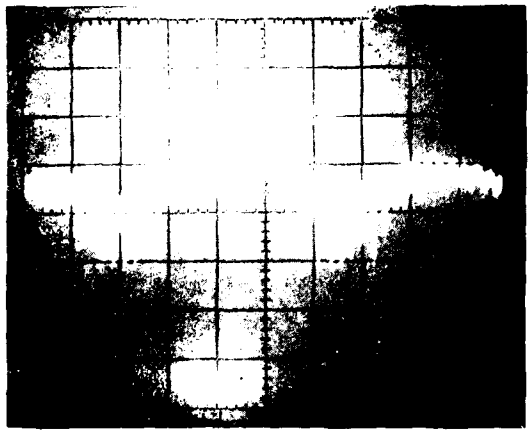

(A) CONVENTIONAL TRANSDUCERS, 0.013-WAVELENGTH-DEEP GROOVES

(B) JOGGED TRANSDUCERS, 0.013-WAVELENGTH-DEEP GROOVES

(C) JOGGED TRANSDUCERS, 0.020-WAVELENGTH-DEEP GROOVES

Figure 17. Resonator Frequency Response

TABLE 7. DELIVERABLE FILTER CHARACTERISTICS

Device Number	Center Frequency (MHz)	Loss (dB)	Bandwidth (kHz)
Goals	70.000	<2	8.0
4	70.149	10.0	7.9
7	70.075	6.8	7.9
9	70.067	7.7	7.9
11	70.062	10.8	11.0
8	70.080	8.4	8.5

the dot array weighting on the reflection coefficient are largest more than 3 MHz from the band center. They cannot be observed directly since this is outside the transducer bandwidth.

3. Multimode Response

The other noticeable problem with the responses shown in Figure 17 is the presence of two resonant modes. In previous devices like those used in the aging study, the transducers are placed so that only one mode is coupled to the interdigital transducers. Adjacent modes are completely decoupled (the transducer is on the nulls of the standing wave) so only one resonance appears in the terminal response. The cavity in the high-Q device is smaller than previous devices; the physical cavity plus weighted reflectors equal the previous cavity alone. Thus, similar performance was expected. The design velocity under the transducers was 8 meters/second low due to a design error, but the cause of the multimode response may be a phase shift in the weighted region. If this weighting technique were useful, further study would be warranted. Care must be taken to keep the cavity small when weighted reflectors are used. These results also show that proper transducer placement is crucial since it can lead to decoupling from the unwanted modes and, therefore, the difference between multimode and single mode operation.

D. DELIVERABLE DEVICES

Five of the resonators described in the preceding subsection were built into one-pole filters and packaged for delivery. The characteristics of these filters are shown in Table 7. The loss is significantly greater than the goal of 2 dB. This deviation is caused by several factors. First, the unloaded Q was not 100,000 due to bulk scattering and packaging in dry nitrogen. This limits the theoretical loss in the filter to 5 dB for most devices and 3.5 dB in number 4. The loss in the inductor further increased this loss 6.5 to 7.0 dB before filter sealing. The seam welding operation added some loss, particularly to devices 4 and 11. Thus, the net filter loss varied from 6.8 to 10.8 dB in the final devices. The response of filter 7 is shown in Figure 18. The shape is smooth and symmetrical as expected.

The near-in out-of-band rejection is limited by the spurious mode to 5 to 10 dB. Beyond this, it is limited to 30 dB by the direct transmission or sidelobes of the reflection coefficient. This falls short of the 40 dB goal. Improving the Q would also improve this performance. Far from resonance, the Q is limited by the packaging. The devices and tuning inductors were mounted with no shielding in a dual in-line package as shown in Figure 19. Direct electromagnetic

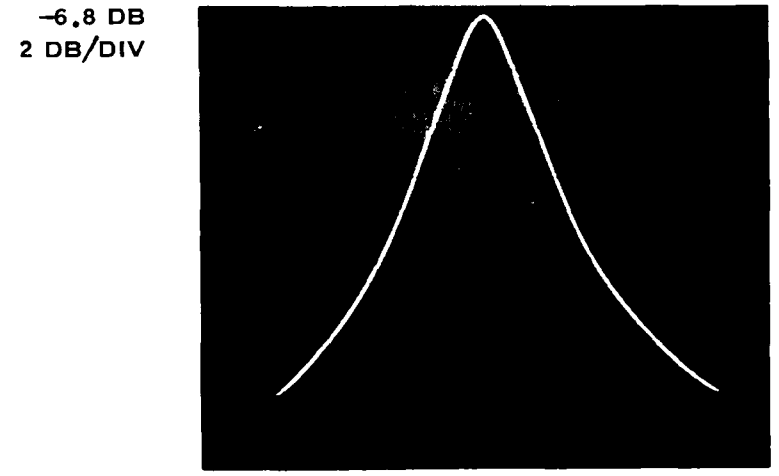

Figure 18. Frequency Response of Filter 7

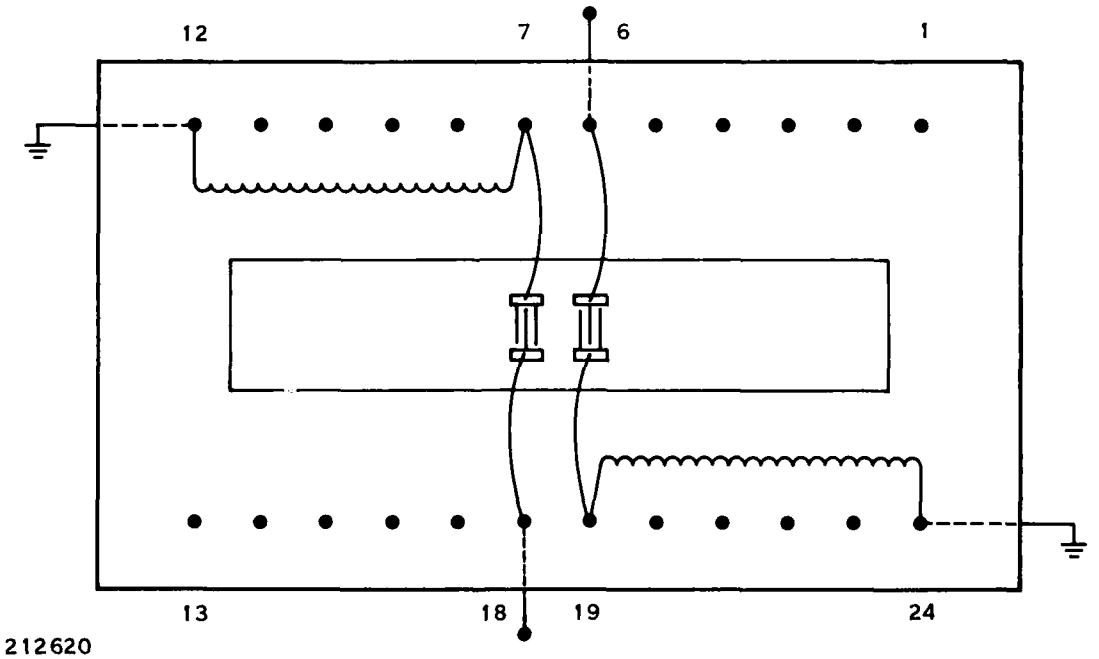

Figure 19. Package and Bonding Diagram for One-Pole Filters

coupling limits the ultimate out-of-band rejection to 40 to 50 dB with further degradation at frequencies. This falls short of the 80-dB goal for ultimate rejection.

E. CONCLUSIONS

The work reported here shows that there is a reasonably good understanding of loss mechanism in resonators. The only weighting techniques for reflectors that are consistent with high-Q operation are groove depth weighting or groove width weighting. The effect of reflection phase changes with these techniques should be examined, especially for filter applications.